Mycobacterium tuberculosis growth arrest on propionate at acidic pH is suppressed by mutations in *phoPR* and pyrazinamide treatment

Heather Murdoch[1,2], Shelby J. Dechow[1,2], Bassel J. Abdalla[1] and Robert B. Abramovitch[1*.]

[1]Department of Microbiology, Genetics & Immunology, Michigan State University, East Lansing, MI,48824

[2]Co-first authors contributed equally to this study.

Disclosures

R.B.A. is an owner of Tarn Biosciences, Inc., a company that is working to develop new antimycobacterial drugs.

***Corresponding Author:**

Robert B. Abramovitch

E-mail: abramov5@msu.edu

Phone: (517) 884-5416

Fax: (517) 353-8957

Abstract

Mycobacterium tuberculosis (Mtb) arrests its growth at acidic pH, when grown on specific single carbon sources, including propionate. To understand the basis of the propionate-driven growth arrest at acidic pH, we conducted a genetic selection for mutants enabling growth on propionate at pH 5.7. All the selected mutants had insertions in the two-component regulatory genes *phoR* or *phoP*. We hypothesized that growth arrest at acidic pH is caused by PhoPR diverting carbon from central carbon metabolism towards lipid anabolism and that when PhoPR is inactivated, growth is promoted through metabolizing propionate by the methyl citrate cycle (MCC) into pyruvate, a permissive carbon source for growth at acidic pH. Using chemical inhibition and mutants of the MCC pathway, we demonstrate that the enhanced growth is dependent on the MCC. Furthermore, stimulating lipid synthesis via the methylmalonyl-CoA pathway by adding Vitamin B12 restricts growth in the *ΔphoPR* mutant and, conversely, restricting lipid anabolism by inhibiting the triacylglycerol (TAG) synthase *tgs1* enhances growth of the *ΔphoPR* mutant. Notably, CoA pools increased in the *ΔphoPR* mutant grown on propionate, directly supporting our model. Given the role of CoA metabolism in pyrazinamide sensitivity, Mtb sensitivity to pyrazinamide was examined on propionate at acidic pH. Surprisingly, pyrazinamide treatment of WT Mtb suppresses growth arrest on propionate at acidic pH. In contrast, the *phoPR* mutant has enhanced sensitivity to pyrazinamide. Together, these findings support that propionate-driven growth arrest at acidic pH is caused by metabolic remodeling that is regulated by PhoPR and is associated with pyrazinamide sensitivity.

Importance

When grown on certain single carbon sources, such as propionate, Mtb arrests its growth at acidic pH and establishes a state of non-replicating persistence (NRP). To understand the genetic basis of this growth restriction, a genetic selection was performed to identify mutants unable to arrest growth at acidic pH with propionate as a sole carbon source. The selection exclusively identified mutants in the PhoPR two-component regulatory system, which functions to modulate cell envelope lipids and redox homeostasis through the upregulation of lipid synthesis at acidic pH. We demonstrate that PhoPR arrests growth at acidic pH by diverting carbon away from the methyl citrate cycle towards lipid anabolism. Surprisingly, treatment of Mtb with pyrazinamide at acidic pH on propionate also enabled growth. These data suggest that drug susceptibility may be impacted by enhanced growth and metabolic capacity of Mtb in acidic and propionate-rich environments, such as within the macrophage or the granuloma.

70 **Introduction**

71 *Mycobacterium tuberculosis* (Mtb) is a slow-growing pathogen that replicates within
72 macrophages or extracellularly. Depending on the conditions, the bacterium may be colonizing
73 environments with specific carbon sources and varying pH. The combinations of pH, carbon
74 source availability, and other environmental cues can impact Mtb growth rate and virulence.
75 During growth *in vitro*, or *in vivo*, Mtb has a slow doubling time of 20 hours to 70 days(1-3). Under
76 low oxygen, starvation, or mildly acidic pH on specific carbon sources, Mtb enters a non-
77 replicating persistent (NRP) state that allows the pathogen to arrest its growth while maintaining
78 its viability(4). Slow or arrested growth in mycobacteria is thought to play a role in establishing
79 tuberculosis-like diseases and can promote phenotypic drug tolerance and persistence(4-7).
80 Therefore, a mechanistic understanding of how Mtb regulates its growth rate, in response to
81 specific environmental cues, is necessary for understanding pathogenesis and characterizing
82 antibiotic susceptibility.

83 One of the key regulators of pH-driven adaptations in Mtb is the PhoPR two-component
84 regulatory system (TCS). PhoPR induces the expression of virulence-related genes in response
85 to acidic pH, magnesium, chloride and CO_2(8-11). These virulence-related genes include the
86 ESX-1 secretion system and cell envelope lipid synthesis genes such as *pks2*, *pks3* and *pks4*
87 which generate sulfolipid (SL) and other acylated trehalose lipids (12, 13). Notably, *phoPR*
88 mutants are highly attenuated in mice and guinea pigs (14, 15), making PhoPR a target for
89 vaccine development(16), supporting that PhoPR and adaptation to acidic pH or related cues are
90 critical for Mtb pathogenesis.

91 Our lab previously discovered that Mtb has restricted growth on specific single carbon
92 sources at acidic pH. Mtb grows well on carbon sources that function at the intersection of
93 glycolysis and the TCA cycle (e.g. pyruvate, acetate, oleic acid and cholesterol)(17). In contrast,
94 on other tested carbon sources, such as glycerol or propionate, Mtb fully arrests its growth at
95 acidic pH and establishes a state of NRP. We refer to this phenotype as acid growth arrest (17,

96 18). We hypothesized that Mtb has evolved means to restrict growth at acidic pH on specific
97 carbon sources to regulate growth and support pathogenesis. Indeed, we previously selected for
98 suppressor mutants of acid growth arrest in *ppe51* that enabled Mtb growth on glycerol at acidic
99 pH, increased its replication in infected activated macrophages, and resulted in decreased
100 fitness(18, 19). The goal of this study is to define the mechanisms of acid growth arrest on
101 propionate as a sole carbon source.

102 Significant research has been conducted examining propionyl-CoA metabolism in Mtb,
103 given it is a catabolic product of cholesterol, a carbon source consumed by Mtb in the host(20).
104 Propionyl-CoA is toxic to Mtb and is detoxified by the methyl citrate cycle (MCC) or by
105 incorporation into methyl branched lipids (such as phthiocerol dimycocerosates (PDIM), SL and
106 acylated trehaloses) (21, 22). The MCC is composed of the methyl-isocitrate lyases *icl1/icl2* along
107 with *prpC* and *prpD* (22). *icl1/icl2, prpC* and *prpD* are essential for growth in minimal media
108 supplemented with propionate (22-25). In the presence of vitamin B12, Mtb is able to survive in
109 the absence of the MCC, by promoting metabolism via methylmalonyl-CoA pathway, enabling the
110 sequestration of propionyl-CoA into methyl branched lipids such as PDIM (21, 22).

111 To define the mechanism of propionate-driven acid growth arrest, we conducted a forward
112 genetic selection for transposon (Tn) mutants that suppress acid growth arrest on propionate at
113 acidic pH. The selection exclusively identified Tn mutants in the PhoPR TCS. Based on these
114 findings, we propose a model where PhoPR arrests growth by diverting propionate towards the
115 synthesis of cell envelope lipids and, when mutated, growth is promoted by metabolism of
116 propionate by the MCC into pyruvate, a permissive carbon source for growth at acidic pH(17).
117 Additionally, we found that pyrazinamide (PZA) treatment also suppresses the acid growth arrest
118 phenotype in WT Mtb and on propionate while PZA selectively sensitizes the *phoPR* mutant to
119 killing PZA. Together, these findings support a model linking acidic pH, carbon source, PhoPR
120 signaling and growth state for PZA activity.

121

Results

PhoPR is required for acid growth arrest on propionate.

We previously reported that Mtb grows on propionate at pH 7.0, but arrests growth on at pH 5.7, based on changes in optical density (17). To determine if Mtb is viable and non-replicating, we examined growth by optical density and CFUs over the course of 12 days of Mtb incubated on propionate or pyruvate at pH 5.7. Mtb arrested growth on propionate (Figure 1A) and was viable (Figure 1B), whereas pyruvate was permissive for growth. Therefore, like acid growth arrest on glycerol, Mtb is non-replicating and viable during propionate-induced acid growth arrest.

We hypothesized that growth arrest on propionate is a regulated process and not intrinsic to the carbon source itself, given that the carbon source can be metabolized at neutral pH and Mtb is viable. To test this hypothesis, a forward genetic selection was performed to identify suppressor mutants of acid growth arrest on propionate at acidic pH. An Mtb Erdman transposon (Tn) mutant library containing ~100,000 mutants was plated on agar plates containing minimal media buffered to pH 5.7 and supplemented with 2mM propionate as a sole carbon source. Mutants with enhanced acidic growth (EAG) phenotype formed colonies on the plates following 8 weeks of incubation. In total, 20 colonies were isolated, and 16 were confirmed as mutants that could grow on propionate (Figure 1C). Using whole genome sequencing or inverse PCR, we identified Tn insertion sites in 12 of the confirmed mutants and all mutants were in *phoR or phoP,* including 6 independent insertions in *phoR and* one insertion in *phoP.* (Supplemental Table 1). Notably, several of the isolated *phoR* mutants also had mutations in the PDIM gene *ppsE*. We confirmed the phenotype of these mutants and observed that the *phoR*::Tn and *phoP*::Tn mutants grew on propionate at acidic pH, with higher growth in the *phoR*::Tn mutant (Figure 1D). Using a *ΔphoPR* deletion mutant and complemented strain previously generated in the CDC1551 background (10), we confirmed that at pH 5.7 on propionate the *ΔphoPR* mutant demonstrated robust growth compared to the wildtype and the phenotype was complemented (Figure 1E). There

148 was no significant difference between strains at neutral pH (Figure S1A). Therefore, we conclude
149 that PhoPR is required for acidic growth arrest on propionate at acidic pH.
150
151 **The *phoPR* mutant has enhanced growth on multiple carbon sources at acidic pH**
152 Previously, we established that *phoPR* is required to slow the growth of Mtb on the
153 permissive carbon source pyruvate at acidic pH(17). Therefore, we sought to determine if *phoPR*
154 is required for growth arrest on other carbon sources. We observed that the *ΔphoPR* mutant
155 displays enhanced growth on specific carbon sources that are permissive for growth at acidic pH
156 (pyruvate and acetate) and normally non-permissive for growth at acidic pH (propionate and
157 succinate), with the strongest enhanced growth phenotype observed in propionate (Figure 2).
158 We previously observed that acid growth arrest on glycerol was dependent on both pH
159 and carbon concentration(19). Therefore, we defined the interactions of pH and propionate
160 concentration on Mtb growth by testing growth at varying pH levels (pH 5.0-7.0), and propionate
161 concentrations (0.16 mM to 20 mM) (Figure 3). This assay was conducted in 96 well plates where
162 Mtb exhibits less robust growth, as compared to standing flask growth conditions used in prior
163 experiments. At 10 mM and 20 mM propionate, the *phoPR* mutant exhibited enhanced growth at
164 pHs 5.0-5.7, (Figure 3 A-C), whereas at pHs 6.0-7.0, the mutant had similar growth to the wild-
165 type. The Δ*phoPR* mutant exhibited a higher OD at 20 mM propionate, suggesting that growth is
166 proportionate to carbon source availability. Therefore, acid growth arrest is induced at pH 5.7 or
167 below. Notably, the PhoPR regulon is strongly induced pH below 6.0(9), consistent with the
168 induction of PhoPR signaling driving the growth arrest phenotype that we see. *pks2* is strongly
169 induced at acidic pH in a *phoPR*-dependent manner and is required for the synthesis of sulfolipids.
170 At acidic pH, we have previously shown that Mtb promotes SL synthesis and accumulation in a
171 *phoPR*-dependent manner(17). We previously isolated a *pks2::*Tn mutant and hypothesized that
172 if enhanced growth is a consequence of diversion of carbon from the TCA cycle, then the *pks2::Tn*
173 mutant should have enhanced growth on propionate. We examined the growth of the WT,

174 *phoR*::Tn and *pks2::*Tn mutants on propionate at acidic pH and observed that the *pks2::*Tn mutant
175 displayed an intermediate impact, with higher growth than the WT, but less than that of the *phoR*
176 mutant (Figure 1D). Therefore, the enhanced growth is also dependent on *pks2*, implicating
177 changes in lipid synthesis or the cell envelope composition in growth arrest.
178
179 **PhoPR is required for acidic pH-dependent cell death**
180 We were surprised to observe the *phoPR* mutant grow on propionate at pH 5.0 (Figure 3A).
181 This highly acidic pH can lead to cell death. Therefore, we examined WT, Δ*phoPR* mutant and
182 complemented strains for growth and viability over a 12-day time course in 2 mM propionate as
183 a sole carbon source, incubated in standing flasks. As anticipated, we observed a significant
184 reduction of WT OD and CFUs at acidic pH, indicating cell death, and an increase of CFUs for
185 the Δ*phoPR* mutant (Figure 4). Therefore, we conclude that cell death at acidic pH, is not an
186 intrinsic stress associated at acidic pH and instead dependent on PhoPR-dependent activities,
187 possibly related to remodeling of metabolism. Notably, the differences in growth between the pH
188 5.0 conditions in the dose response study (Figure 3A) and this experiment, are likely driven be
189 different conditions in the 96-well plates and standing flasks, where we see more robust growth
190 in standing flasks.
191
192 **PhoPR restricts growth at acidic pH by diverting carbon from the methyl citrate cycle**
193 One of the key functions of PhoPR at acidic pH is envelope composition remodeling by
194 promoting lipid synthesis, including sulfolipids (SL), diacyltrehaloses (DAT) and
195 polyacyltrehaloses (PAT)(13). Deletion of *phoPR* results in a near complete loss of SL at acidic
196 pH, which is compensated for by the induction of triacylglycerol (TAG) (17). Propionyl-CoA is an
197 important substrate for the PhoPR-dependent synthesis of methyl-branched lipids such as SL,
198 DAT and PAT, as well as methyl-branched lipids synthesized independently of PhoPR, such as
199 PDIM and TAG. Given the partially enhanced growth of the *pks2* mutant (Figure 1D), we

200 hypothesized that growth arrest at acidic pH is due to PhoPR diverting carbon away from central
201 metabolism towards lipid metabolism, thus starving Mtb of carbon needed for growth. Indeed, a
202 similar phenomenon has been observed for hypoxia-driven growth arrest and the induction of *tgs1*
203 to produce TAG (26). We further hypothesize that in the PhoPR mutant, the propionate can be
204 metabolized into pyruvate via the methyl citrate cycle (MCC). Pyruvate is permissive for growth
205 at acidic pH, thus the redirection of propionate from lipid anabolism (in the WT) to pyruvate via
206 the MCC (in the *phoPR* mutant) could explain the enhanced growth of the Δ*phoPR* mutant on
207 propionate at acidic pH.

208 To first test this model, we examined if the MCC was required for growth on propionate at
209 acidic pH, using mutants in the methylisocitrate lyases *icl1/icl2* and complemented strains(24).
210 Lacking a *phoPR* mutant in the *icl1/icl2* mutant backgrounds, we used a chemical inhibitor of
211 *phoPR* signaling, ethoxzolamide (ETZ) (27), to downregulate PhoPR. The strains were cultured
212 in minimal media in propionate with or without ETZ, at acidic pH, and growth and viability were
213 monitored over 12 days (Figures 5A and S2A). In the DMSO control, the WT and *icl1* or *icl2*
214 mutants all had arrested growth at acidic pH, and the *icl1/icl2* exhibited a reduction of CFUs and
215 OD, a phenotype consistent with propionate toxicity in the absence of the MCC (Figure 5A and
216 S2A). In the ETZ-treated cells, we observed enhanced growth of the WT, consistent with PhoPR
217 inhibition driving growth at acidic pH (Figures 5A and S2A). The *icl2* mutant had a stronger
218 phenotype which could be driven by the direct regulation of Icl2 by propionate(28). Notably, at pH
219 7.0, the single *icl1* or *icl2* mutants grew well on propionate in both the DMSO and ETZ treated
220 cells, while the icl1/icl2 mutant could not grow, due to propionate toxicity (Figure S3). To further
221 confirm the role of the MCC in *phoPR*-dependent enhanced growth, we examined if chemical
222 inhibition of icl1/2 by itaconic acid (ITA) could inhibit the enhanced growth. Indeed, ITA completely
223 inhibited Mtb *phoPR* mutant growth on propionate at acidic pH (Figure S4). These data are
224 consistent with the MCC being required for enhanced growth of the Δ*phoPR* mutant at acidic pH.

225 To further validate the model that PhoPR-dependent diversion of carbon to lipid synthesis
226 promotes the growth arrest phenotype, we hypothesized that stimulating lipid synthesis in the
227 PhoPR mutant would suppress growth on propionate. To test this hypothesis, we examined
228 whether the induction of the methylmalonyl-CoA pathway, by the supplementation with vitamin
229 B12, reduces the growth of the PhoPR mutant. The WT, Δ*phoPR*, and complement strains were
230 grown in minimal media at acidic pH supplemented with propionate, with or without vitamin B12,
231 and growth and viability were monitored. As hypothesized, vitamin B12 suppresses the growth
232 of the Δ*phoPR* mutant at acidic pH (Figure 5B and S2B), supporting that stimulating lipid
233 anabolism suppresses growth at acidic pH on propionate. Addition of vitamin B12 had no impact
234 on Mtb growth at pH 7.0 on propionate , in the WT or Δ*phoPR* mutant (Figure S2D), supporting
235 the phenotypes are acidic pH dependent.
236 Mtb increases the production of the TAG when *phoPR* is deleted, possibly as a
237 mechanism to balance redox homeostasis(17). We hypothesized that TAG synthesis may function
238 similarly as a sink for carbon and slow the growth of WT or the Δ*phoPR* mutant. To test this
239 hypothesis, we used a DosRST inhibitor, MSU-43996, that potently inhibits *tgs1* expression and
240 TAG synthesis (29). We examined the growth of WT, and the Δ*phoPR* mutant in the presence of
241 propionate, with or without 40 μM MSU-43996 at acidic pH and neutral pH (Figure 5C and S1B) .
242 When *tgs1* is inhibited, the WT exhibits enhanced growth, and the Δ*phoPR* mutant exhibits further
243 enhanced growth at acidic pH (Figure 5C and S2C); while no major differences are observed at
244 neutral pH (Figure S1B). These data further reinforce the hypothesis that lipid synthesis is slowing
245 or arresting Mtb growth at acidic pH.
246
247 **PhoPR restricts free CoA at acidic pH**
248 We hypothesize that if PhoPR is diverting carbon away from central metabolism to slow growth,
249 this adaptation may be associated with less available free CoA in the WT at acidic pH. In the
250 Δ*phoPR* mutant, metabolism of propionate into pyruvate would fuel the TCA cycle and promote

251 increases in free CoA pools. To test this hypothesis, we examined total free CoA in the WT,
252 Δ*phoPR* mutant, and complemented strains in 2mM propionate, 10 mM pyruvate or 10 mM
253 glycerol at pH 5.7. During growth arrest in propionate and glycerol, WT CoA pools remained
254 relatively stable over the course of six days (Figures 6A and S5). In contrast, on propionate CoA
255 pools in the Δ*phoPR* mutant increased threefold at day 3 and then lowered again at day 6 (Figure
256 6A). There is no change between day 0 and 6 in CoA in the growth arrested Δ*phoPR* mutant in
257 the presence of glycerol (Figure S5). In pyruvate, which is growth permissive, CoA pools
258 increased slightly in the WT and were enhanced in the Δ*phoPR* mutant, which also has enhanced
259 growth in pyruvate (Figure 6C). Consistent with our hypothesis, diversion of carbon from the TCA
260 cycle to lipid synthesis by the addition of vitamin B12, decreases the accumulation of CoA in the
261 Δ*phoPR* mutant (Figure 6B), which is also associated with decreased growth (Figure 5B).

262 In our findings, free CoA in the Δ*phoPR* mutant on propionate at acidic pH is negatively
263 associated with stimulation of lipid synthesis pathways and positively associated with growth. The
264 decrease in CoA pools at Day 6 in the Δ*phoPR* mutant suggested that additional lipid synthesis
265 pathways may be engaged over time. The cultures are grown in standing flasks and we anticipate
266 that growth over 6 days by the Δ*phoPR* mutant will consume oxygen and induce the *dosRST*
267 pathway. This would cause the strong induction of the TAG-synthase *tgs1* and provide an induced,
268 second mechanism to restrict growth under the hypoxic conditions caused by the growth of the
269 mutant. To test this hypothesis, we examined the impact of the *dosRST* inhibitor MSU-39446, on
270 CoA pools. In the MSU-39446 treated Δ*phoPR* mutant the CoA pools did not decrease at day 6
271 (Figure 6D), a phenotype consistent with the enhanced growth caused by MSU-39446 treatment
272 (Figure 5C). Notably, CoA pools increased in the WT, a response consistent with the enhanced
273 growth of the WT (Figure 5C). Together, these data further support the hypothesis that growth
274 arrest on propionate at acidic pH is driven by restriction of central metabolism via synthesis of
275 PhoPR-dependent lipids.

276

277 **Pyrazinamide suppresses growth arrest on propionate at acidic pH.**

278 Pyrazinamide (PZA) activity is enhanced at acidic pH and its mechanism of action is
279 uncertain, but recent data suggests it may be associated with CoA metabolism and cell envelope
280 lipid homeostasis (17, 30-32). Therefore, we hypothesized that the WT strain and Δ*phoPR* mutant
281 may exhibit differential sensitivity to PZA. To test this hypothesis, we examined the sensitivity of
282 WT, Δ*phoPR* mutant, and complemented strains to PZA across a dose range from 0-100 μM in
283 minimal medium supplemented with 2mM propionate at pH 5.7. Surprisingly, following 21 days of
284 incubation, PZA at concentrations of 2.5 and 5 μM suppressed acid growth arrest in the WT and
285 complemented strains (Figure 7A). However, the Δ*phoPR* mutant was growth arrested under
286 these conditions, showing that it has enhanced sensitivity to PZA (as compared to the DMSO
287 control, where the Δ*phoPR* mutant grew robustly). At a concentration of 1.25 μM, the growth of
288 the WT and Δ*phoPR* mutant are about equal (Figure 7A) ,suggesting a complex interplay between
289 PZA concentration and modulation of growth at acidic pH on propionate.

290 The above assay was conducted in 96-well plates, and we sought to better characterize
291 the suppression of acid growth arrest by PZA in a standing flask-based acid growth arrest assay,
292 which exhibits more robust growth. WT, Δ*phoPR* mutant and complemented strains were
293 incubated at pH 5.7 with propionate as a sole carbon source, treated with 3.8 μM PZA, 20 μM
294 isoniazid (INH), or a DMSO control, and growth was monitored over 12 days. The WT and
295 complemented strains exhibited enhanced growth on PZA as compared to DMSO (Figure 7B-7E),
296 whereas the Δ*phoPR* mutant was killed by PZA and showed robust growth in the DMSO control
297 (Figure 7B-7E). We hypothesized that like enhanced growth of the Δ*phoPR* mutant, that PZA may
298 also be causing enhanced growth by inhibiting lipid synthesis. To test this hypothesize, we
299 examined if additional of vitamin B12, limited the enhanced growth of PZA treated WT Mtb. As
300 hypothesized, vitamin B12 blocked the enhanced growth in the PZA treated Mtb (Figures S6 and
301 S7). INH inhibited the growth of all of the strains, showing the differential growth impact is PZA-
302 specific (Figure 7F and 7G). We also examined the impact of PZA sensitivity on the strains grown

303 on pyruvate and observed that that WT Mtb did not exhibit enhanced growth on PZA, showing the
304 enhanced growth is propionate specific. (Figure S8). Notably, the Δ*phoPR* was also mores
305 sensitive to PZA on pyruvate (Figure S8), supporting that the enhanced PZA sensitivity is not
306 carbon source specific. To determine if the enhanced growth on WT Mtb on PZA is shared
307 between different strains, we also conducted this experiment in Mtb Erdman. We observed that
308 3.8 μM PZA caused enhanced growth of WT Erdman (Figure S9). No significant differences were
309 observed, between strains or treatments, when the experiment was replicated at neutral pH
310 (Figure S10), an expected result given the acidic pH-dependent activity of PZA. Together, these
311 findings show that PZA can result in enhanced growth or killing of Mtb depending on the pH,
312 concentration of PZA and PhoPR-signaling of the bacterium. This discovery generates further
313 complexity for understanding the mechanism of PZA function, as pH and carbon sources can vary
314 in different environments during infection, and differences in *phoPR* or *prpR* genotype and
315 function exist in clinical strains (33-35).
316
317 **Discussion**
318 Mtb remodels its physiology at acidic pH below ~6.5, demonstrating several pH-dependent
319 adaptations associated with pathogenesis and drug susceptibility(5, 36). Changes in carbon
320 metabolism are a substantial component of acidic pH-dependent adaptations. We and others
321 have observed that Mtb restricts its ability to grow on specific carbon sources at acidic pH (17,
322 37, 38), a phenomenon we refer to as acid growth arrest. Previously, we found that Mtb arrests
323 its growth on glycerol and that this growth arrest is overcome by mutations *in ppe51* that promote
324 enhanced glycerol uptake (36). We concluded that growth arrest is overcome by increasing
325 glycerol uptake (36), possibly to overcome reduced glyceraldehyde-3-phosphate dehydrogenase
326 activity at acidic pH(37). *ppe51* mutants did not promote growth on other non-permissive carbon
327 sources, including propionate, leading us to hypothesize that acid growth arrest has different
328 mechanisms for different carbon sources.

329 The isolation of *phoPR* Tn mutants that can grow on propionate strongly support our
330 hypothesis of carbon source specific metabolic restraints at acidic pH (Figure 8). For example,
331 *phoPR* mutants cannot grow on glycerol and *ppe51* EAG variants cannot grow on propionate.
332 Given that the Δ*phoPR* mutant does not have enhanced growth on many carbon sources (Figure
333 2), the enhanced growth is not likely solely dependent on enhanced permeability due to defects
334 in the cell envelope. Together, multiple independent observations support that the growth arrest
335 on propionate is due to the diversion of carbon towards the synthesis of PhoPR-dependent lipids
336 (Figure 8). For example, growth arrest is observed at acidic pH when methyl-branched lipid
337 synthesis pathways are activated on propionate, and when PhoPR-dependent pathways (SL, DAT
338 and PAT), DosRST-dependent pathways (TAG), or vitamin B12-dependent pathways (PDIM) are
339 available to the pathogen. Disruption of these pathways by deletion of *phoPR* (Fig. 8), interruption
340 of the *phoPR*-regulated gene SL synthesis gene *pks2* (Fig. 1*)*, inhibition of PhoPR-by treatment
341 with ETZ (Fig. 5), inhibition of *tgs1* expression by treatment with MSU-39446 (Fig. 5), or the
342 absence of vitamin B12, results in the enhanced acid growth phenotype. Notably, treatment with
343 PZA also leads to enhanced acid growth, suggesting part of PZA function may be related to
344 inhibiting lipid synthesis. When lipid synthesis is blocked, growth on propionate at acidic pH is
345 dependent on the MCC, which is one of primary mechanisms by which Mtb detoxifies propionate
346 (39). Pyruvate is a permissive carbon source at acidic pH, therefore, it is expected that if
347 propionate is metabolized to pyruvate via the MCC that it would promote growth (Figure 8).
348 Mtb induces PhoPR at acidic pH on various carbon sources (glycerol, pyruvate,
349 propionate), and WT Mtb has a functional MCC, therefore, we do not believe that PhoPR is
350 induced specifically to detoxify propionate. Rather, we observed that the PhoPR mutant
351 experiences reductive stress at acidic pH, and we hypothesize that lipid synthesis serves the
352 purpose of oxidizing cofactors (such as NADPH to NADP+) to maintain redox homeostasis(17,
353 18). Consistent with this hypothesis, we observe that downregulation of SL production in the
354 *phoPR* mutant is associated with induction of other lipids such as TAG (17). Blocking both PhoPR

355 and DosRST pathways removes four of the major lipid synthesis pathways (SL, DAT, PAT and
356 TAG) and results in the most robust growth of propionate (Figure 5C, S2C). Pyruvate is known to
357 promote growth at acidic pH, and we hypothesize that by entering the TCA cycle near the
358 anaplerotic node provides Mtb the metabolic flexibility to maintain redox homeostasis by
359 balancing anabolism and catabolism, possibly via the PEP glyoxylate cycle(40, 41). In this
360 manner, if propionate is not diverted to lipid synthesis, it can be turned into a permissive carbon
361 source that balances redox homeostasis at the anaplerotic node, even in the absence of *phoPR*.
362 Similar to the mutations in *phoPR*, PZA at low concentrations can also suppress Mtb
363 growth arrest on propionate at acidic pH. Based on our model for propionate-dependent growth
364 arrest, we reason that PZA treatment may be acting to inhibit lipid synthesis, thus enabling more
365 propionate to be metabolized by the MCC into central metabolism. The mechanism of action of
366 PZA remains controversial, but recent evidence supports a role for CoA metabolism and changes
367 in cell envelope lipid synthesis playing a role in its activity (30, 42) . Resistance mutations to PZA
368 arise in PanD, which is involved in the synthesis of CoA. The PZA metabolite POA can bind to
369 PanD to inhibit CoA synthesis (32). Reduced CoA levels are predicted to result in lower levels of
370 lipid synthesis, as it is an essential cofactor in the initial steps of fatty acid activation. Notably, it
371 was recently reported that PDIM genes are strongly downregulated by treatment with PZA (43)
372 and PDIM mutants are associated with resistance to PZA (42). Therefore, we speculate enhanced
373 growth of the WT is due to reduced PDIM synthesis or other long-chain fatty acids that require
374 CoA for their synthesis. The small range of concentrations where this enhanced growth in the WT
375 is observed (~3 μM) may reflect a hypomorphic phenotype, where CoA metabolism is sufficiently
376 repressed by PZA to impact lipid metabolism, but not so much so to fully deplete CoA and kill the
377 cell. It is surprising that the PhoPR mutant is susceptible to PZA and does not have further
378 enhanced growth. We speculate that an alternative mechanism is driving PZA sensitivity in the
379 *phoPR* mutant, possibly differential expression of a *phoPR* pathway independent on lipid
380 anabolism. For example, a *ppe51* loss of function mutant is reported to have enhanced

susceptibility to PZA(44). *ppe51* is downregulated in the *phoPR* mutant, suggesting it, or some other unknown PhoPR-regulated genes may play a role in susceptibility that overcomes the expected further enhanced growth. Alternatively, the *phoPR* mutant may have increased permeability due to changes in the cell envelope. It is possible that this increased permeability is increasing the intracellular concentration of PZA, accumulating to sufficient levels to inhibit growth.

Concluding remarks

The observation that PhoPR restricts growth on propionate at acidic pH is analogous to the findings of Baek at al, who showed that the DosRST and hypoxia regulated gene *tgs1* inhibits growth during hypoxia by diverting carbon from the TCA cycle(26). In both cases, growth restriction is an environmental adaption and not an inherent metabolic limitation. TB disease is caused by slow growing mycobacteria and persistence and growth arrest are associated with drug tolerance. By understanding the complex mechanisms by which Mtb integrates environmental cues, metabolism and growth arrest, we may define new drug targets that can disrupt pathogenesis in a way the increases bacterial growth. Enhanced growth is associated with reduced fitness in macrophages (36) and enhanced drug susceptibility *in vitro* (18). Therefore, these non-traditional drug targets may have unique impacts during treatment, including treatment shortening. Indeed, PZA was essential to shortening TB treatment times to six months and it is tempting to speculate that some of this activity may be related to PZA enhancing Mtb growth in mildly acidic and cholesterol rich environments, such as the macrophage or the granuloma. It is also important to consider that *phoPR* and *prpR* have variants in clinical isolates (33-35), supporting that the interplay of PhoPR and propionate observed in these studies, maybe associated with differential pathogenesis and drug susceptibility and in human infections and drug treatment.

407 **Materials and Methods**

408 **Bacterial strains and growth**

409 Mtb experiments were conducted with WT ERDMAN or WT CDC1551 as indicated. The Δ*phoPR*
410 deletion mutant, and complemented strains are in the CDC1551 background (10) and the *icl1/2*
411 mutants and complemented strains are in the Erdman background(24). Cultures were maintained
412 in 7H9 media supplemented with 10% OADC and .05% Tween-80. All single carbon source
413 experiments were performed in MMAT minimal media buffered to acidic pH 5.7 or pH 7.0(21),
414 using (1 g l−1 KH2PO4, 2.5 g l−1 Na2PO4, 0.5 g l−1 (NH4)2SO4, 0.15 g l−1 asparagine, 10 mg l−1
415 MgSO4, 50 mg l−1 ferric ammonium citrate, 0.1 mg l−1 ZnSO4, 0.5 mg l−1 CaCl2, and 0.05%
416 Tyloxapol) . For 12-day growth experiments, time points were taken every three days. For each
417 of our growth curve experiments, 2mM propionate was used unless stated otherwise. Chemical
418 inhibitors and supplements were used at the following concentrations: Ethoxzolamide at 40 μM,
419 MSU-39446 at 40 μM, Itaconic acid at 2 mM and vitamin B12 at 10ug/ml. Mtb was seeded in T-
420 25 standing tissue culture flasks in 8ml of minimal media at an initial cell density of 0.05 OD and
421 incubated at 37 °C and 5% CO_2. 500 μL of each culture was taken each day for optical density
422 measurements. Bacterial viability was assessed enumerating colony-forming units (CFUs) on
423 7H10+OADC plates.

424

425 **Genetic selection**

426 Transposon mutagenesis was performed in Mtb Erdman using the ϕMycoMarT7 Tn system as
427 previously described(45), generating a library with ~100,000 Tn mutants. The Tn mutant library
428 was plated on MMAT pH 5.7 agar plates supplemented with 2mM propionate as the sole carbon
429 source. Plates were incubated at 37°C, with mutants appearing around week 8 and isolated for
430 growth. Single-colony isolates were confirmed as EAG (enhanced acidic growth) mutants under
431 acidic conditions in liquid media MMAT pH 5.7 supplemented with 2mM propionate. The

432 transposon insertion sequences were confirmed using inverse PCR (46) or whole genome
433 sequencing.
434
435 **Whole Genome Sequencing**
436 Genomic DNA of selected mutants as well as the WT Erdman control was isolated, DNA libraries
437 were constructed, and sequenced using the Illumina MiSeqm in-paired end, 250 bp read format
438 (PE250). After the sequencing run, reads were demultiplexed and converted to FASTQ format
439 using the illumina bcl2 fastq (v1.8.4) script. The reads in the raw data files were then subjected
440 to trimming of low-quality bases and removal of adapter sequences using Trimmomatic v0.36,
441 with a 4 bp sliding window, and a read quality cutoff of below 15 or read length cutoff less than 36
442 bp. The trimmed reads were then aligned to the Erdman reference genome using the Burrow-
443 Wheeler alignments. Genome analysis tool kit base quality score recalibration, indel alignment,
444 and duplicate removal were applied, and SNP and INDEL discovery were performed.
445
446 **pH and propionate dose response combination growth assays**
447 Mtb cultures were incubated in a range of pH-buffered MMAT media ranging from pH 5.0-7.0 at a
448 starting OD of 0.2 in 96 well plates. Cultures were treated with a 2.5-fold serial dilution (0mM-
449 20mM) of propionate and incubated over a course of 21 days, with growth assessed by optical
450 density.
451
452 **Free CoA assay**
453 Free CoA was measured using a commercially available assay (Sigma-Aldrich). Cultures were
454 maintained in 7H9, and then seeded to an OD of 0.2 and resuspended in minimal media
455 supplemented with 2mM propionate in 8 ml of media. Free CoA was measured at Day 0, 3, and
456 6 and concentration determined using a standard curve.
457

458 **Pyrazinamide Sensitivity Assays.**

459 Dose response assays were conducted in a 96 well plate cultures seeded at OD 0.2 and in
460 minimal media supplemented with 2mM propionate across a dose response from 100 μM-0 μM
461 of PZA. Plates were incubated for 6 days in a sealed Ziploc bag at 37C and OD read on a plate
462 reader. Standing flask assays were conducted using conditions as described earlier in the
463 methods. WTCDC, Δ*phoPR* mutant, and complement were grown in minimal media at acidic pH
464 supplemented with propionate and treated with DMSO, 3.84 uM Pyrazinamide, and 20uM
465 Isoniazid using conditions described above. Growth was measured Day 0, 3, 6, 9, and 12.
466 Viability was measured Day 0 and Day 12 by enumerating CFUs.

467

468

469 **Acknowledgements**

470 We thank Prof. John McKinney for sharing the *icl1/icl2* mutant strains. Research on this project
471 was supported by grants from the NIAID (R01 AI116605 and R01 AI150855) and AgBioResearch.

472

473

474 **Figure Legends**

475 **Figure 1. PhoPR arrests growth on propionate at acidic pH**. A) Growth curves of WT Mtb CDC
476 strain grown in acidic pH for 12 days, in media supplemented with propionate or pyruvate. B)
477 Bacterial viability evaluated using CFUs plated at days 0 and 12, demonstrating the viability of
478 the growth-arrested bacteria under propionate. C) Relative growth of 16 different transposon
479 mutants with enhanced growth on propionate relative to the WT (dotted line). All sequenced
480 mutants were in *phoR or phoP* (Supplemental Table 1). D) Growth curves of transposon mutants
481 in *phoR*, *phoP* and *pks2*, grown at acidic pH in minimal media supplemented with 2mM
482 propionate. E) Growth curves of Δ*phoPR* mutant and complemented strain compared to WT CDC
483 strain showing growth of the *phoPR* mutant. Multiple comparison unpaired t-test was used for the
484 growth curves analysis while one-way ANOVA was used for the viability analysis, * <0.05, **
485 <0.01, *** <0.001, **** <0.0001. Experiments were replicated at least twice with similar results.
486

487 **Figure 2. PhoPR enhances growth on specific carbon sources at acidic pH.** Mtb growth was
488 evaluated on various carbon sources after 21 days incubation. The Δ*phoPR* mutant exhibits
489 enhanced growth at acidic pH on selected permissive (acetate and pyruvate) and non-permissive
490 carbon sources (propionate and succinate). Two-way ANOVA was used for statistical analysis, *
491 <0.05, ** <0.01, *** <0.001, **** <0.0001. Experiments were replicated at least twice with similar
492 results.
493

494 **Figure 3. Enhanced growth of the Δ*phoPR* mutant is dependent on level of pH and**
495 **propionate concentration.** Growth of the Δ*phoPR* mutant, the WT and complemented strains
496 was tested in minimal media supplemented with a range of concentrations of propionate (20 mM
497 to 0.16 mM) at different pHs (5.0-7-.0). The Δ*phoPR* mutant has enhanced growth in dependent
498 on propionate concentration at pHs of 5.0, 5.5 and 5.7 (**A-C**), but not 6-7 (**D-F**). A multiple

499 comparison unpaired t-test was used for this analysis, * <0.05, ** <0.01, *** <0.001, **** <0.0001.
500 Experiments were replicated at least twice with similar results.
501
502 **Figure 4. PhoPR is required for cell death at pH 5.0. A)** The WT, Δ*phoPR* mutant, and
503 complemented strain were incubated at acidic pH for 12 days, in minimal media supplemented
504 with propionate. The Δ*phoPR* mutant has enhanced growth compared to the WT, a phenotype
505 that is complemented. **B)** Viability assays, show that the WT and complemented strains exhibit
506 cell death at pH 5.0, while the *phoPR* mutant grows. A multiple comparison unpaired t-test was
507 used for this analysis, * <0.05, ** <0.01, *** <0.001, **** <0.0001. Experiments were replicated at
508 least twice with similar results.
509 **Figure 5. PhoPR restricts growth at acidic pH by diverting carbon from the methyl citrate**
510 **cycle. A)** Growth curves of the WT, knockout strain of isocitrate lyases 1 and/or 2, and the
511 complemented strains, treated with DMSO or ethoxzolamide (ETZ), an indirect inhibitor of PhoPR,
512 showing a significant reduction in growth in the *icl2* and double knockout strains. **B)** Growth
513 curves conducted in wildtype, *phoPR* mutant, and complemented strains in minimal media
514 buffered to pH 5.7 supplemented with 2mM propionate and Vitamin B12 over a course of 12 days,
515 showing vitamin B12 suppresses enhanced growth in the Δ*phoPR* mutant strain.**C)** Growth of the
516 WT, Δ*phoPR* mutant, and complement strains treated with MSU-43996 or the DMSO control,
517 showing a enhanced growth in the presence of MSU-43996 treatment. An unpaired t-test was
518 used between individual groups and the WT for the growth curves, while a one-way ANOVA was
519 used for the viability experiments, * <0.05, ** <0.01, *** <0.001, **** <0.0001. Experiments were
520 replicated at least twice with similar results.
521
522 **Figure 6: Enhanced acid growth is associated with increased free CoA pools. A)** Free CoA
523 pools in the Δ*phoPR* mutant, WT CDC, and complemented strain grown in minimal media

524 supplemented with 2 mM propionate at acidic pH, showing enhanced metabolic capacity (i.e.,
525 higher free CoA pools) in the Δ*phoPR* mutant during the first three days of growth (p = 0.006),
526 which significantly decreases around day 6 (p = 0.009). **B)** Free CoA pools in the three strains,
527 grown in minimal media supplemented with vitamin B12 at acidic pH, showing no significant
528 differences between the three strains throughout the 6-day growth period. **C)** Free CoA pools in
529 the three strains, grown in minimal media supplemented with 10 mM of pyruvate at acidic pH,
530 showing enhanced metabolic capacity of the Δ*phoPR* mutant and WT through day 6. **D)** Free CoA
531 pools in the three strains, grown in minimal media supplemented with 40 μM of MSU-43996 at
532 acidic pH, showing enhanced metabolic capacity of the Δ*phoPR* mutant when *tgs1*, a is inhibited.
533 Two-way ANOVA was used for this analysis, * <0.05, ** <0.01, *** <0.001, **** <0.0001.
534 Experiments were replicated at least twice with similar results.
535
536 **Figure 7: PZA suppresses acid growth arrest on propionate. A)** Dose-response relationship
537 of pyrazinamide (100-0 μM) in the Δ*phoPR* null mutant, WT, and complement strains, conducted
538 in minimal media supplemented with 2mM propionate at acidic pH, demonstrating enhanced
539 growth of the WT and complemented strains on PZA at concentrations between 5.0-2.5 μM. **B**
540 **and C)** Assessment of the growth (B) and Viabilty (C) of the three strains in minimal media
541 supplemented with 2mM propionate at acidic pH, treated with the vehicle as a control, showing
542 enhanced growth of the Δ*phoPR* mutant. **D and E)** Assessment of the growth (D) and viability (E)
543 of the three strains in minimal media supplemented with 2mM propionate at acidic pH treated with
544 PZA (3.84 μM), demonstrating enhanced growth of the WT and higher sensitivity of the Δ*phoPR*
545 mutant. **F and G)** Assessment of the growth (F) and viability (G) of the three strains in minimal
546 media supplemented with 2mM propionate at acidic pH treated with isoniazid (INH, 20 μM),
547 demonstrating similar levels of sensitivity in the three strains. Multiple comparison T-test was used

548 for the growth curves analysis, while Two-way ANOVA was used for the viability, * <0.05, ** <0.01,
549 *** <0.001, **** <0.0001. Experiments were replicated at least twice with similar results.
550
551 **Figure 8: Model for Mtb growth arrest on propionate at acidic pH and mechanisms of**
552 **suppression by mutations in *phoPR* or pyrazinamide treatment.** Propionate-dependent acid
553 growth arrest is a PhoPR-regulated response driven by diversion of carbon away from central
554 metabolism and into the synthesis lipids. At acidic pH, propionyl-CoA is used as a substrate to
555 synthesize methyl-branched lipids, either through the polyketide synthases Pks2, Pks3 and Pks4,
556 or through the methyl-malonyl pathway. Additionally, the enzyme MutAB, a vitamin B12-
557 dependent enzyme, catalyzes the reversible interconversion between malonyl-CoA and succinyl-
558 CoA, contributing to the synthesis of branched lipids. In either cases, low pH triggers remodeling
559 of central metabolism towards complex lipids synthesis to alter the mycomembrane structure as
560 a pH-dependent adaptation, consuming the CoA pools and slowing, or arresting growth in the
561 process. This pH-dependent adaptation in lost in the *phoPR* null mutant or under indirect PhoPR
562 chemical inhibition using ethoxzolamide (ETZ). Instead, the propionate is metabolized into
563 pyruvate by the methylcitrate cycle, a permissive carbon source, increasing CoA pools and
564 permitting fast growth. Additionally, at acidic pH, the *phoPR* null mutant upregulates triacylglycerol
565 synthesis using tgs1. Chemical inhibition of *tgs1* using MSU-39446 prevents diversion of CoA
566 pools into TAG synthesis and away from central metabolism, increasing CoA pools, metabolism
567 and growth in both the WT and *phoPR* null mutant. PZA treatment causes enhanced growth in
568 the WT, which may be driven by inhibiting lipid synthesis via depletion of CoA pools.
569

570 **References**

571

572 1. Gill WP, Harik NS, Whiddon MR, Liao RP, Mittler JE, Sherman DR. 2009. A replication
573 clock for Mycobacterium tuberculosis. Nat Med 15:211-4.

574 2. Rohde KH, Veiga DF, Caldwell S, Balazsi G, Russell DG. 2012. Linking the transcriptional
575 profiles and the physiological states of Mycobacterium tuberculosis during an extended
576 intracellular infection. PLoS Pathog 8:e1002769.

577 3. Munoz-Elias EJ, Timm J, Botha T, Chan WT, Gomez JE, McKinney JD. 2005. Replication
578 dynamics of Mycobacterium tuberculosis in chronically infected mice. Infect Immun
579 73:546-51.

580 4. Zheng H, Abramovitch RB. 2019. Host-pathogen interactions influencing Mycobacterium
581 tuberculosis persistence and drug tolerance *In* Lewis K (ed), Persister Cells and Infectious
582 Disease. Springer.

583 5. Baker JJ, Dechow SJ, Abramovitch RB. 2019. Acid Fasting: Modulation of Mycobacterium
584 tuberculosis Metabolism at Acidic pH. Trends Microbiol 27:942-953.

585 6. Adams KN, Takaki K, Connolly LE, Wiedenhoft H, Winglee K, Humbert O, Edelstein PH,
586 Cosma CL, Ramakrishnan L. 2011. Drug tolerance in replicating mycobacteria mediated
587 by a macrophage-induced efflux mechanism. Cell 145:39-53.

588 7. Liu Y, Tan S, Huang L, Abramovitch RB, Rohde KH, Zimmerman MD, Chen C, Dartois V,
589 VanderVen BC, Russell DG. 2016. Immune activation of the host cell induces drug
590 tolerance in Mycobacterium tuberculosis both in vitro and in vivo. J Exp Med 213:809-25.

591 8. Walters SB, Dubnau E, Kolesnikova I, Laval F, Daffe M, Smith I. 2006. The *Mycobacterium*
592 *tuberculosis* PhoPR two-component system regulates genes essential for virulence and
593 complex lipid biosynthesis. Molecular Microbiology 60:312-330.

594 9. Abramovitch RB, Rohde KH, Hsu FF, Russell DG. 2011. *aprABC*: a *Mycobacterium*
595 *tuberculosis* complex-specific locus that modulates pH-driven adaptation to the
596 macrophage phagosome. Mol Microbiol 80:678-94.

597 10. Tan S, Sukumar N, Abramovitch RB, Parish T, Russell DG. 2013. Mycobacterium
598 tuberculosis Responds to Chloride and pH as Synergistic Cues to the Immune Status of
599 its Host Cell. PLoS Pathog 9:e1003282.

600 11. Dechow SJ, Goyal R, Johnson BK, Haiderer ER, Abramovitch RB. 2025. Carbon dioxide
601 regulates Mycobacterium tuberculosis PhoPR signaling and virulence. Infect Immun
602 93:e0056824.

603 12. Feng L, Chen S, Hu Y. 2018. PhoPR Positively Regulates whiB3 Expression in Response
604 to Low pH in Pathogenic Mycobacteria. J Bacteriol 200.

605 13. Asensio JG, Maia C, Ferrer NL, Barilone N, Laval F, Soto CY, Winter N, Daffe M, Gicquel
606 B, Martin C, Jackson M. 2006. The virulence-associated two component PhoP-PhoR

607 system controls the biosynthesis of polyketide-derived lipids in *Mycobacterium*
608 *tuberculosis*. Journal of Biological Chemistry 281:1313-1316.

609 14. Perez E, Samper S, Bordas Y, Guilhot C, Gicquel B, Martin C. 2001. An essential role for
610 *phoP* in *Mycobacterium tuberculosis* virulence. Molecular Microbiology 41:179-187.

611 15. Martin C, Williams A, Hernandez-Pando R, Cardona PJ, Gormley E, Bordat Y, Soto CY,
612 Clark SO, Hatch GJ, Aguilar D, Ausina V, Gicquel B. 2006. The live *Mycobacterium*
613 *tuberculosis phoP* mutant strain is more attenuated than BCG and confers protective
614 immunity against tuberculosis in mice and guinea pigs. Vaccine 24:3408-3419.

615 16. Luabeya AKK, Rozot V, Imbratta C, Ratangee F, Shenje J, Tameris M, Mendelsohn SC,
616 Geldenhuys H, Fisher M, Musvosvi M, Young C, Mulenga H, Bilek N, Mabwe S, Jelsbak
617 IM, Rodriguez E, Puentes E, Doce J, Aguilo N, Martin C, Pillay C, Tait D, Russell M, Van
618 Der Merve A, Rutkowski K, Hunt D, Ginsberg A, Scriba TJ, Hatherill M, team A. 2025. Live-
619 attenuated Mycobacterium tuberculosis vaccine, MTBVAC, in adults with or without M
620 tuberculosis sensitisation: a single-centre, phase 1b-2a, double-blind, dose-escalation,
621 randomised controlled trial. Lancet Glob Health 13:e1030-e1042.

622 17. Baker JJ, Johnson BK, Abramovitch RB. 2014. Slow growth of Mycobacterium
623 tuberculosis at acidic pH is regulated by phoPR and host-associated carbon sources. Mol
624 Microbiol 94:56-69.

625 18. Baker JJ, Abramovitch RB. 2018. Genetic and metabolic regulation of Mycobacterium
626 tuberculosis acid growth arrest. Sci Rep 8:4168.

627 19. Dechow SJ, Baker JJ, Murto M, Abramovitch RB. 2022. ppe51 Variants Enable Growth of
628 Mycobacterium tuberculosis at Acidic pH by Selectively Promoting Glycerol Uptake. J
629 Bacteriol 204:e0021222.

630 20. VanderVen BC, Fahey RJ, Lee W, Liu Y, Abramovitch RB, Memmott C, Crowe AM, Eltis
631 LD, Perola E, Deininger DD, Wang T, Locher CP, Russell DG. 2015. Novel inhibitors of
632 cholesterol degradation in Mycobacterium tuberculosis reveal how the bacterium's
633 metabolism is constrained by the intracellular environment. PLoS Pathog 11:e1004679.

634 21. Lee W, VanderVen BC, Fahey RJ, Russell DG. 2013. Intracellular Mycobacterium
635 tuberculosis exploits host-derived fatty acids to limit metabolic stress. J Biol Chem
636 288:6788-800.

637 22. Savvi S, Warner DF, Kana BD, McKinney JD, Mizrahi V, Dawes SS. 2008. Functional
638 characterization of a vitamin B-12-dependent methylmalonyl pathway in *Mycobacterium*
639 *tuberculosis*: Implications for propionate metabolism during growth on fatty acids. Journal
640 of Bacteriology 190:3886-3895.

641 23. Gould TA, van de Langemheen H, Munoz-Elias EJ, McKinney JD, Sacchettini JC. 2006.
642 Dual role of isocitrate lyase 1 in the glyoxylate and methylcitrate cycles in Mycobacterium
643 tuberculosis. Mol Microbiol 61:940-7.

644 24. Munoz-Elias EJ, McKinney JD. 2005. Mycobacterium tuberculosis isocitrate lyases 1 and
645 2 are jointly required for in vivo growth and virulence. Nat Med 11:638-44.

646 25. Upton AM, McKinney JD. 2007. Role of the methylcitrate cycle in propionate metabolism
647 and detoxification in Mycobacterium smegmatis. Microbiology 153:3973-82.

648 26. Baek SH, Li AH, Sassetti CM. 2011. Metabolic regulation of mycobacterial growth and
649 antibiotic sensitivity. PLoS Biol 9:e1001065.

650 27. Johnson BK, Colvin CJ, Needle DB, Mba Medie F, Champion PA, Abramovitch RB. 2015.
651 The Carbonic Anhydrase Inhibitor Ethoxzolamide Inhibits the Mycobacterium tuberculosis
652 PhoPR Regulon and Esx-1 Secretion and Attenuates Virulence. Antimicrob Agents
653 Chemother 59:4436-45.

654 28. Bhusal RP, Jiao W, Kwai BXC, Reynisson J, Collins AJ, Sperry J, Bashiri G, Leung IKH.
655 2019. Acetyl-CoA-mediated activation of Mycobacterium tuberculosis isocitrate lyase 2.
656 Nat Commun 10:4639.

657 29. Zheng H, Williams JT, Aleiwi B, Ellsworth E, Abramovitch RB. 2020. Inhibiting
658 Mycobacterium tuberculosis DosRST Signaling by Targeting Response Regulator DNA
659 Binding and Sensor Kinase Heme. ACS Chem Biol 15:52-62.

660 30. Thiede JM, Dillon NA, Howe MD, Aflakpui R, Modlin SJ, Hoffner SE, Valafar F, Minato Y,
661 Baughn AD. 2021. Pyrazinamide Susceptibility Is Driven by Activation of the SigE-
662 Dependent Cell Envelope Stress Response in Mycobacterium tuberculosis. mBio
663 13:e0043921.

664 31. Gopal P, Gruber G, Dartois V, Dick T. 2019. Pharmacological and Molecular Mechanisms
665 Behind the Sterilizing Activity of Pyrazinamide. Trends Pharmacol Sci 40:930-940.

666 32. Gopal P, Yee M, Sarathy J, Low JL, Sarathy JP, Kaya F, Dartois V, Gengenbacher M, Dick
667 T. 2016. Pyrazinamide Resistance Is Caused by Two Distinct Mechanisms: Prevention of
668 Coenzyme A Depletion and Loss of Virulence Factor Synthesis. ACS Infect Dis 2:616-626.

669 33. Liu Q, Zhu J, Dulberger CL, Stanley S, Wilson S, Chung ES, Wang X, Culviner P, Liu YJ,
670 Hicks ND, Babunovic GH, Giffen SR, Aldridge BB, Garner EC, Rubin EJ, Chao MC,
671 Fortune SM. 2022. Tuberculosis treatment failure associated with evolution of antibiotic
672 resilience. Science 378:1111-1118.

673 34. Malaga W, Payros D, Meunier E, Frigui W, Sayes F, Pawlik A, Orgeur M, Berrone C,
674 Moreau F, Mazeres S, Gonzalo-Asensio J, Rengel D, Martin C, Astarie-Dequeker C,
675 Mourey L, Brosch R, Guilhot C. 2023. Natural mutations in the sensor kinase of the PhoPR
676 two-component regulatory system modulate virulence of ancestor-like tuberculosis bacilli.
677 PLoS Pathog 19:e1011437.

678 35. Hicks ND, Yang J, Zhang X, Zhao B, Grad YH, Liu L, Ou X, Chang Z, Xia H, Zhou Y, Wang
679 S, Dong J, Sun L, Zhu Y, Zhao Y, Jin Q, Fortune SM. 2018. Clinically prevalent mutations
680 in Mycobacterium tuberculosis alter propionate metabolism and mediate multidrug
681 tolerance. Nat Microbiol 3:1032-1042.

682 36. Dechow SJ, Abramovitch RB. 2024. Targeting Mycobacterium tuberculosis pH-driven
683 adaptation. Microbiology (Reading) 170.

684 37. Gouzy A, Healy C, Black KA, Rhee KY, Ehrt S. 2021. Growth of Mycobacterium
685 tuberculosis at acidic pH depends on lipid assimilation and is accompanied by reduced
686 GAPDH activity. Proc Natl Acad Sci U S A 118.

687 38. Healy C, Ehrt S, Gouzy A. 2024. An exacerbated phosphate starvation response triggers
688 Mycobacterium tuberculosis glycerol utilization at acidic pH. mBio
689 doi:10.1128/mbio.02825-24:e0282524.

690 39. Savvi S, Warner DF, Kana BD, McKinney JD, Mizrahi V, Dawes SS. 2008. Functional
691 characterization of a vitamin B12-dependent methylmalonyl pathway in Mycobacterium
692 tuberculosis: implications for propionate metabolism during growth on fatty acids. J
693 Bacteriol 190:3886-95.

694 40. Munoz-Elias EJ, McKinney JD. 2006. Carbon metabolism of intracellular bacteria. Cell
695 Microbiol 8:10-22.

696 41. Sauer U, Eikmanns BJ. 2005. The PEP-pyruvate-oxaloacetate node as the switch point
697 for carbon flux distribution in bacteria. FEMS Microbiol Rev 29:765-94.

698 42. Gopal P, Sarathy JP, Yee M, Ragunathan P, Shin J, Bhushan S, Zhu J, Akopian T, Kandror
699 O, Lim TK, Gengenbacher M, Lin Q, Rubin EJ, Gruber G, Dick T. 2020. Pyrazinamide
700 triggers degradation of its target aspartate decarboxylase. Nat Commun 11:1661.

701 43. Ostrer L, Crooks TA, Howe MD, Vo S, Jia Z, Hegde P, Schacht N, Aldrich CC, Baughn AD.
702 2025. Mechanism of the Dual Action Self-Potentiating Antitubercular Drug
703 Morphazinamide. bioRxiv doi:10.1101/2024.10.08.617272.

704 44. Bellerose MM, Proulx MK, Smith CM, Baker RE, Ioerger TR, Sassetti CM. 2020. Distinct
705 Bacterial Pathways Influence the Efficacy of Antibiotics against Mycobacterium
706 tuberculosis. mSystems 5.

707 45. Long JE, DeJesus M, Ward D, Baker RE, Ioerger T, Sassetti CM. 2015. Identifying
708 essential genes in Mycobacterium tuberculosis by global phenotypic profiling. Methods
709 Mol Biol 1279:79-95.

710 46. Ochman H, Gerber AS, Hartl DL. 1988. Genetic applications of an inverse polymerase
711 chain reaction. Genetics 120:621-3.
712

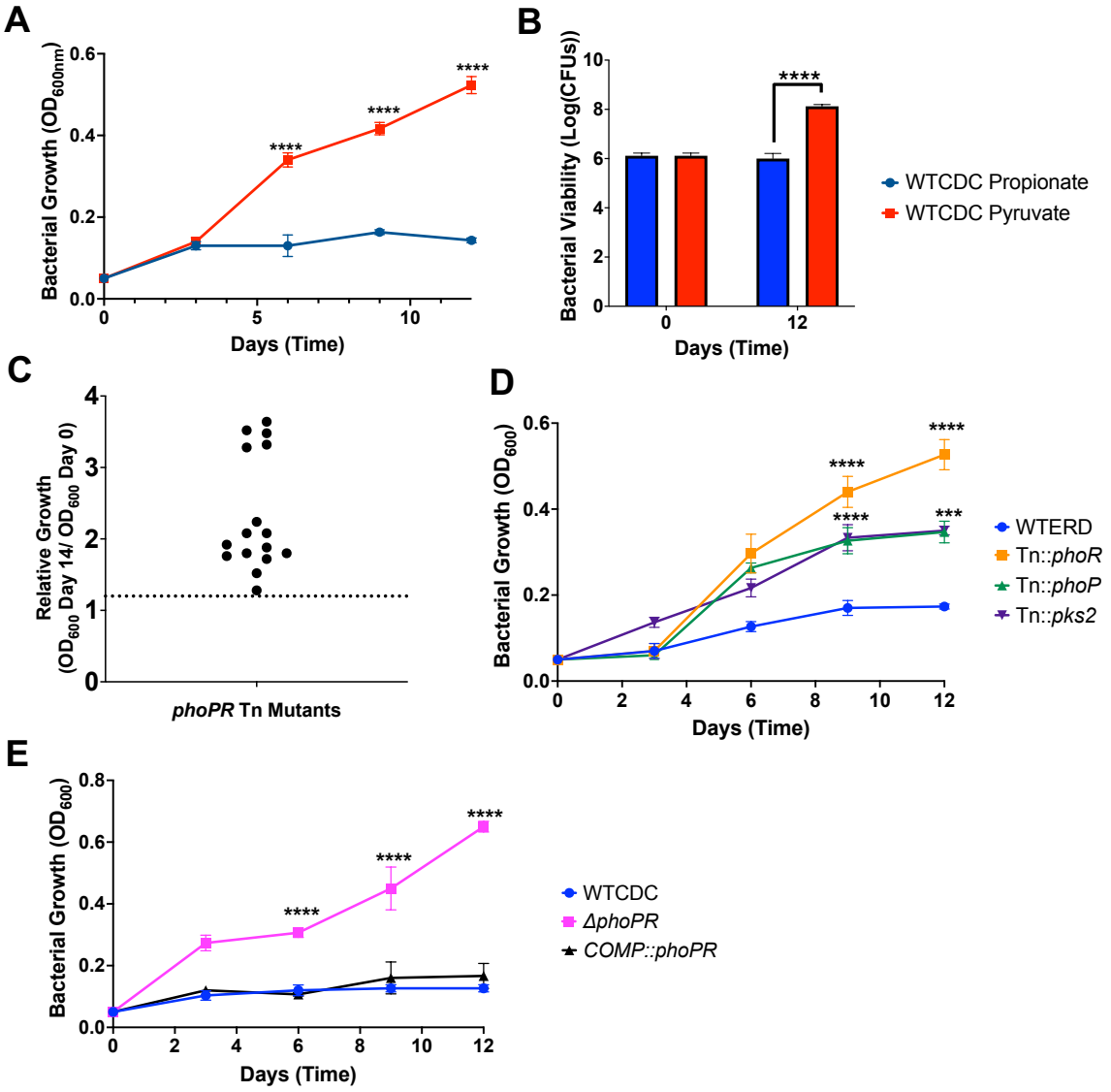
A
Bacterial Growth (OD600nm)
0.0
0.2
0.4
0.6
0
5
10
Days (Time)
****
****
****
B
Bacterial Viability (Log(CFUs))
0
2
4
6
8
10
0
12
Days (Time)
****
WTCDC Propionate
WTCDC Pyruvate
C
Relative Growth
(OD600 Day 14/ OD600 Day 0)
0
1
2
3
4
phoPR Tn Mutants
D
Bacterial Growth (OD600)
0.0
0.2
0.4
0.6
0
2
4
6
8
10
12
Days (Time)
****
****
****
***
WTERD
Tn::phoR
Tn::phoP
Tn::pks2
E
Bacterial Growth (OD600)
0.0
0.2
0.4
0.6
0.8
0
2
4
6
8
10
12
Days (Time)
****
****
****
WTCDC
ΔphoPR
COMP::phoPR

Figure 1

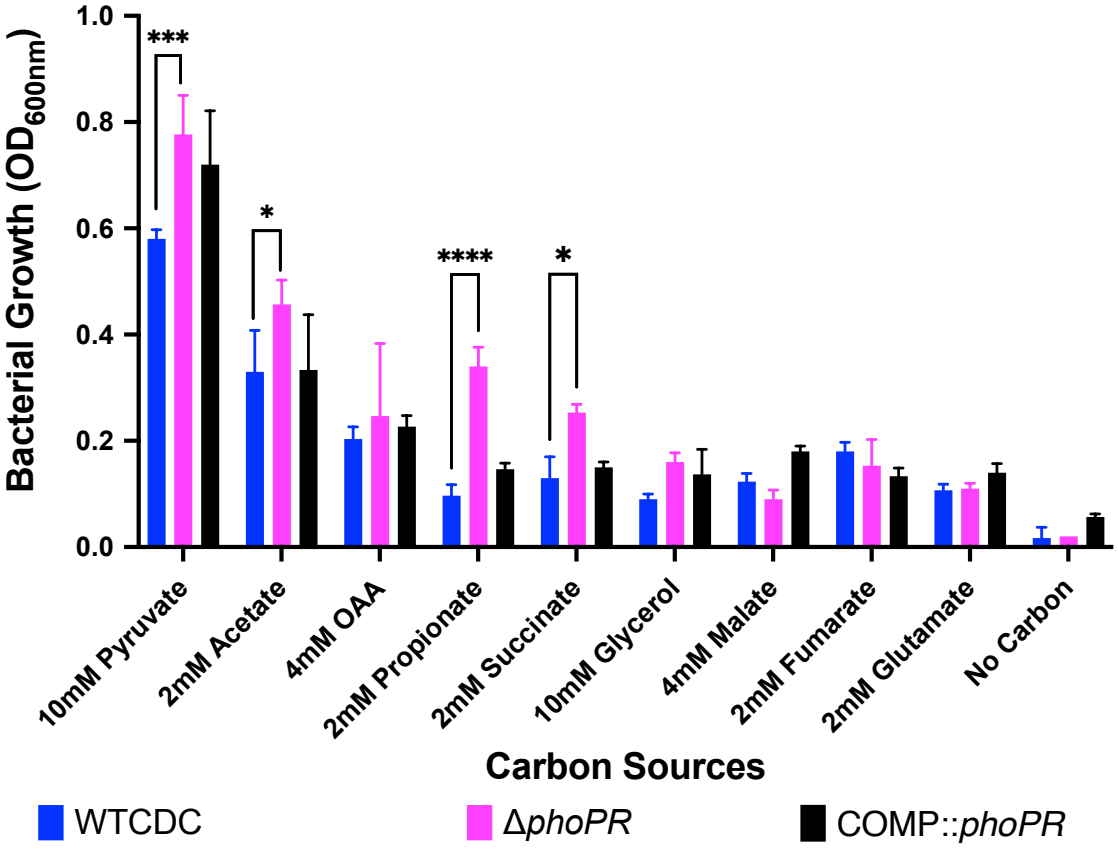
Bacterial Growth (OD_{600nm})
1.0
0.8
0.6
0.4
0.2
0.0
***
*
****
*
10mM Pyruvate
2mM Acetate
4mM OAA
2mM Propionate
2mM Succinate
10mM Glycerol
4mM Malate
2mM Fumarate
2mM Glutamate
No Carbon
Carbon Sources
WTCDC
Δ*phoPR*
COMP::*phoPR*

Figure 2

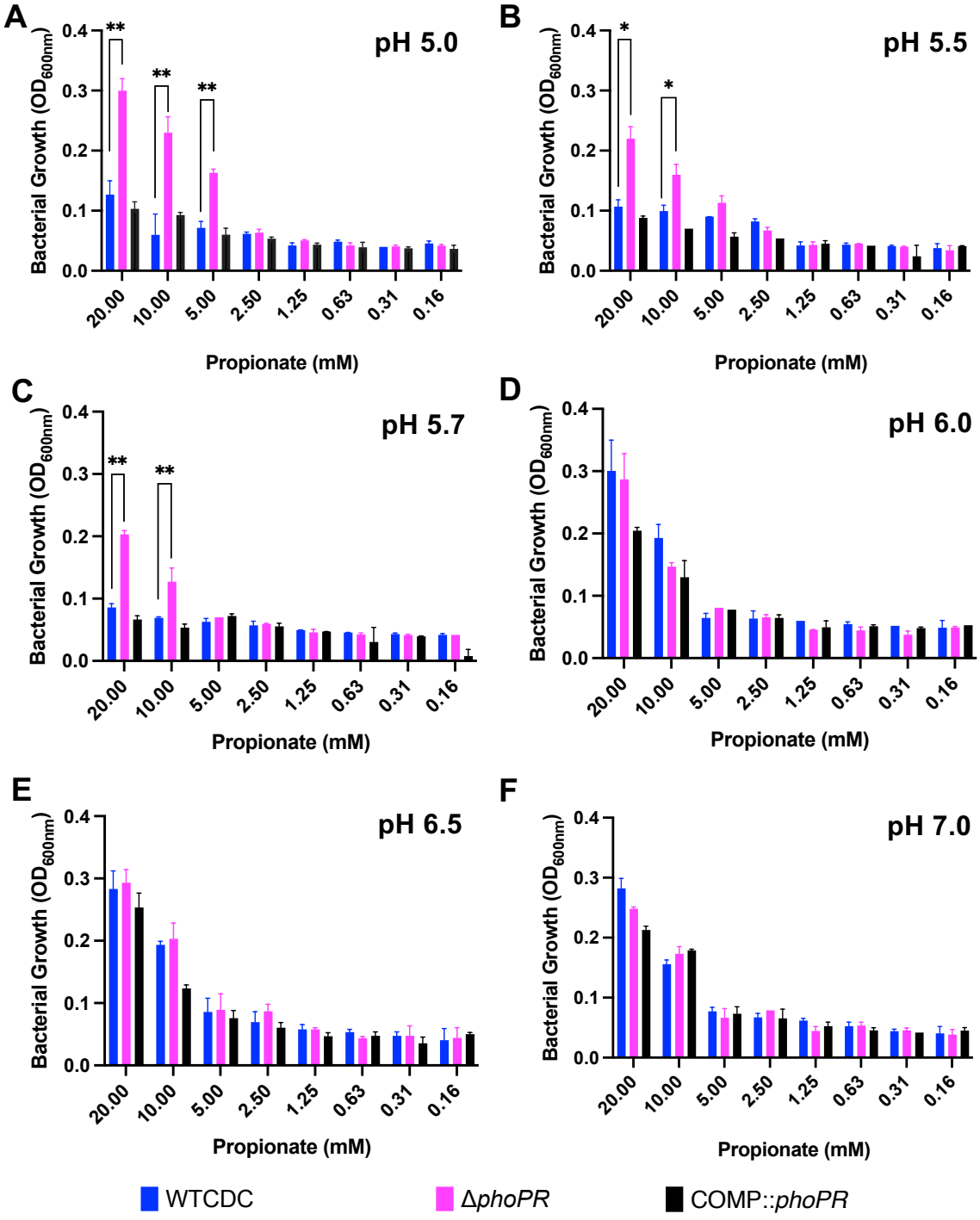
A
pH 5.0
B
pH 5.5
C
pH 5.7
D
pH 6.0
E
pH 6.5
F
pH 7.0
Bacterial Growth (OD_{600nm})
Propionate (mM)
20.00
10.00
5.00
2.50
1.25
0.63
0.31
0.16
WTCDC
ΔphoPR
COMP::phoPR

Figure 3

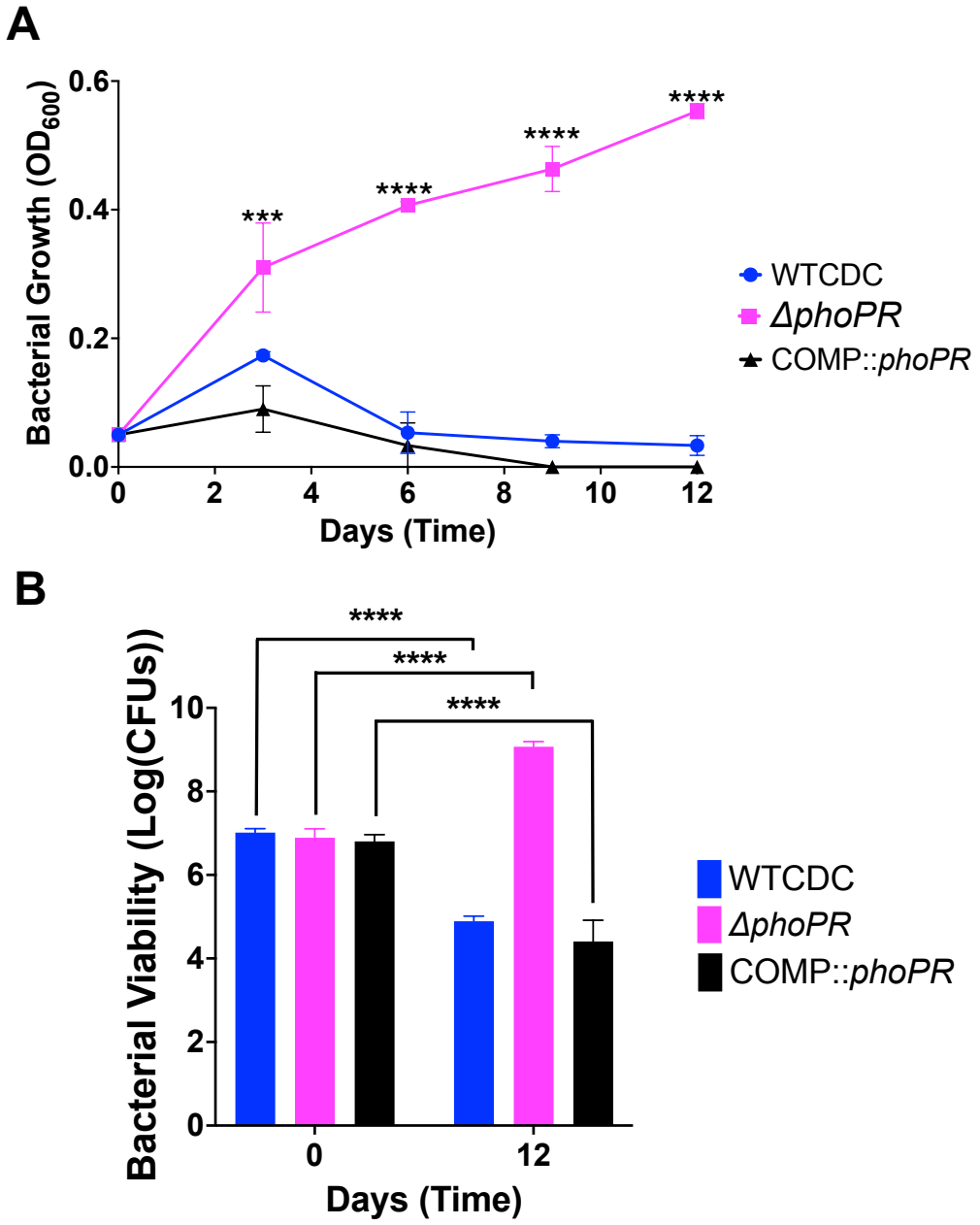
A
Bacterial Growth (OD600)
0.6
0.4
0.2
0.0
0
2
4
6
8
10
12
Days (Time)
***
****
****
****
WTCDC
ΔphoPR
COMP::phoPR
B
Bacterial Viability (Log(CFUs))
10
8
6
4
2
0
0
12
Days (Time)
****
****
****
WTCDC
ΔphoPR
COMP::phoPR

Figure 4

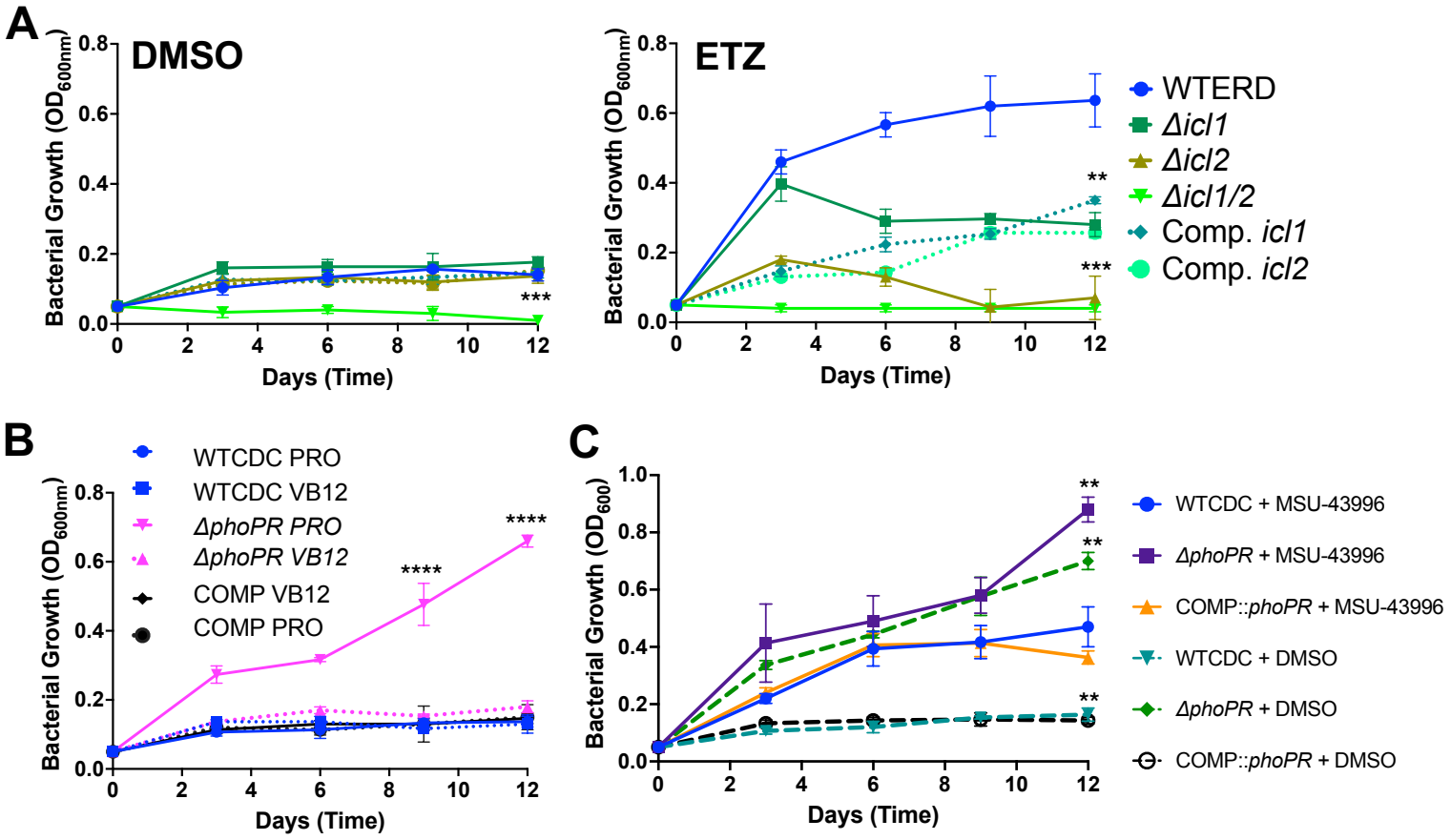
A
DMSO
ETZ
Bacterial Growth (OD600nm)
Days (Time)
WTERD
Δicl1
Δicl2
Δicl1/2
Comp. icl1
Comp. icl2
***
**
B
WTCDC PRO
WTCDC VB12
ΔphoPR PRO
ΔphoPR VB12
COMP VB12
COMP PRO
****
C
Bacterial Growth (OD600)
WTCDC + MSU-43996
ΔphoPR + MSU-43996
COMP::phoPR + MSU-43996
WTCDC + DMSO
ΔphoPR + DMSO
COMP::phoPR + DMSO

Figure 5

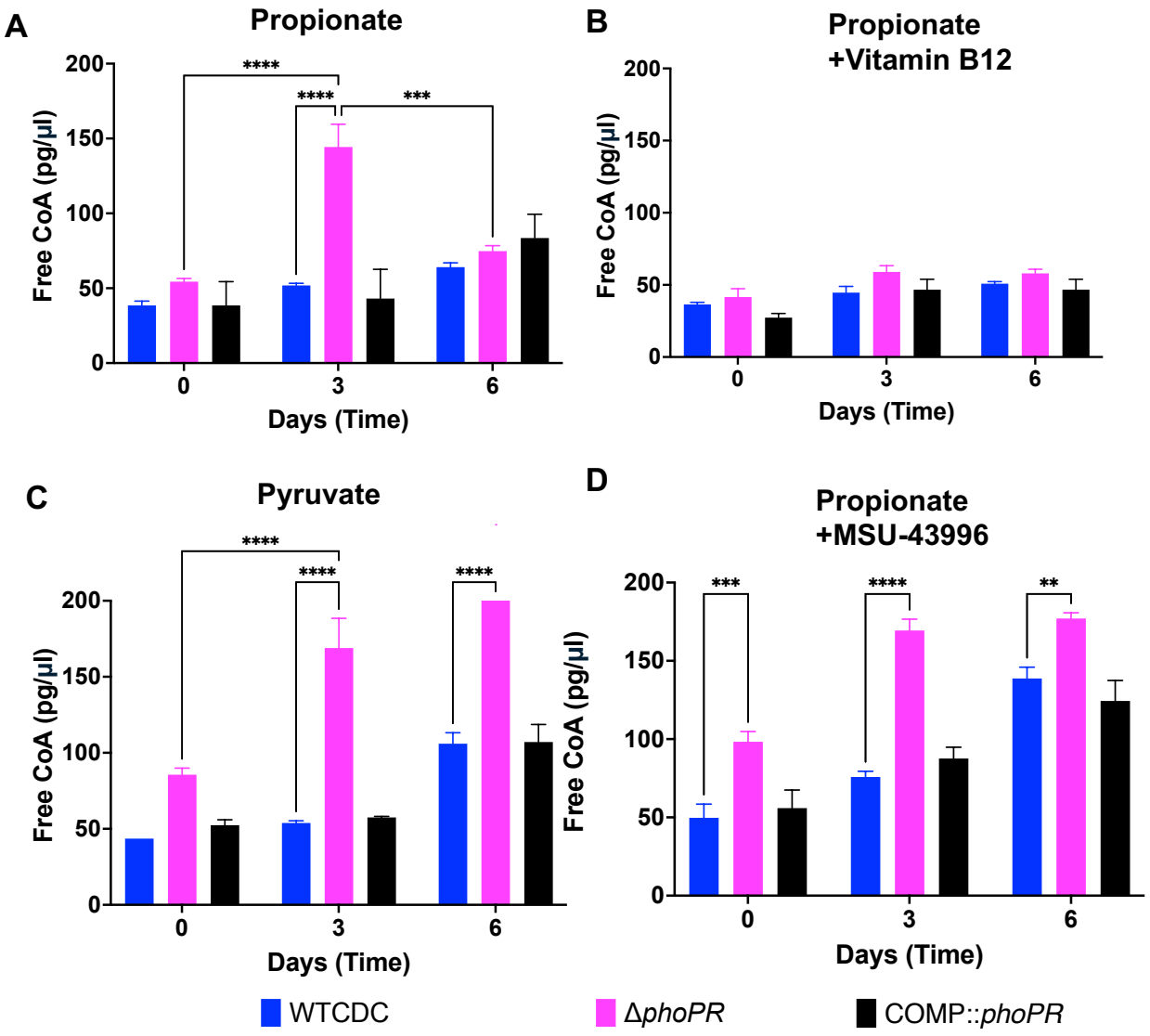
A
Propionate
Free CoA (pg/µl)
200
150
100
50
0
****
****
***
0
3
6
Days (Time)
B
Propionate
+Vitamin B12
Free CoA (pg/µl)
200
150
100
50
0
0
3
6
Days (Time)
C
Pyruvate
Free CoA (pg/µl)
200
150
100
50
0
****
****
****
0
3
6
Days (Time)
D
Propionate
+MSU-43996
Free CoA (pg/µl)
200
150
100
50
0
***
****
**
0
3
6
Days (Time)
WTCDC
ΔphoPR
COMP::phoPR

Figure 6

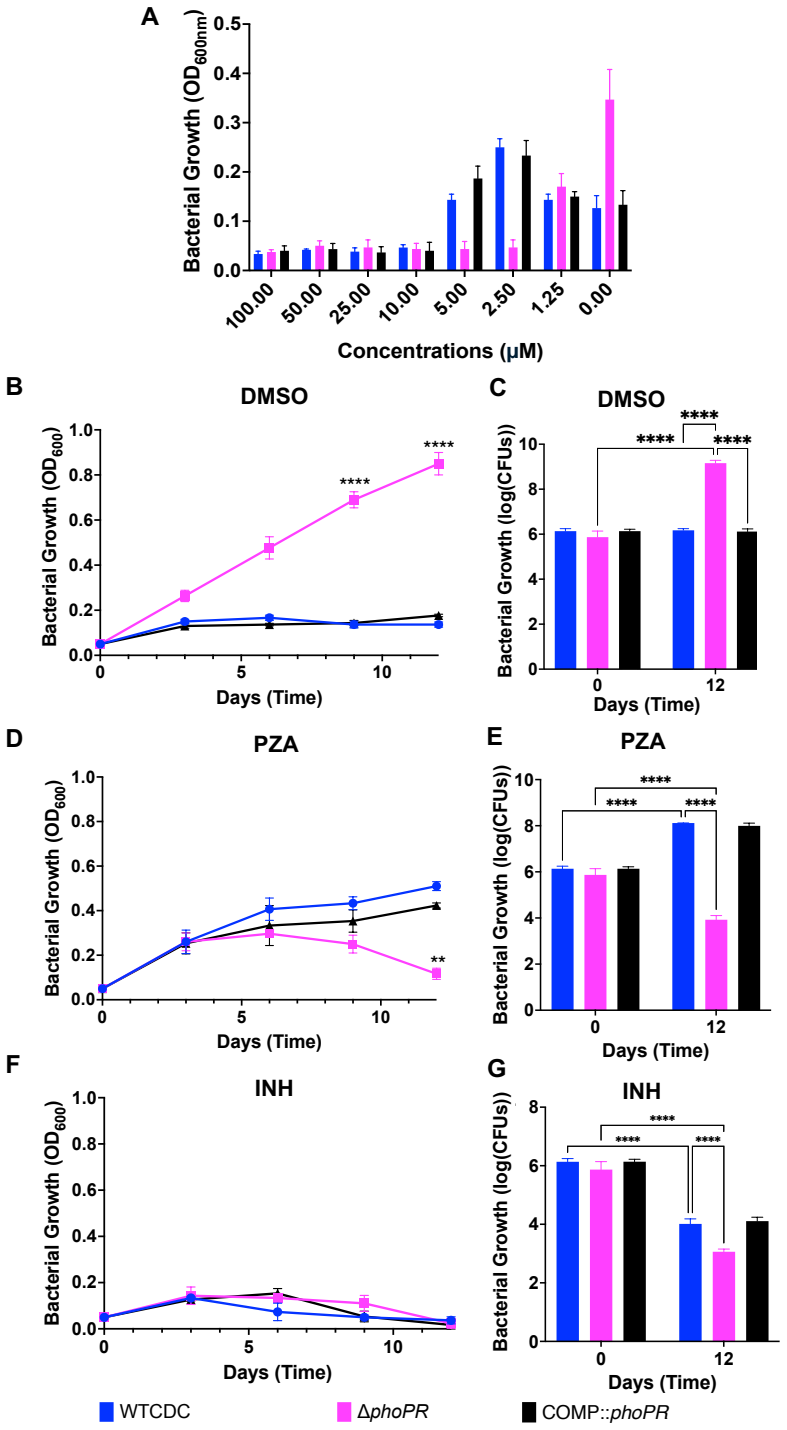
A
Bacterial Growth (OD600nm)
0.5
0.4
0.3
0.2
0.1
0.0
100.00
50.00
25.00
10.00
5.00
2.50
1.25
0.00
Concentrations (μM)
B
DMSO
Bacterial Growth (OD600)
1.0
0.8
0.6
0.4
0.2
0.0
****
****
0
5
10
Days (Time)
C
DMSO
Bacterial Growth (log(CFUs))
10
8
6
4
2
0
****
****
****
0
12
Days (Time)
D
PZA
Bacterial Growth (OD600)
1.0
0.8
0.6
0.4
0.2
0.0
**
0
5
10
Days (Time)
E
PZA
Bacterial Growth (log(CFUs))
10
8
6
4
2
0
****
****
****
0
12
Days (Time)
F
INH
Bacterial Growth (OD600)
1.0
0.8
0.6
0.4
0.2
0.0
0
5
10
Days (Time)
G
INH
Bacterial Growth (log(CFUs))
8
6
4
2
0
****
****
****
0
12
Days (Time)
WTCDC
ΔphoPR
COMP::phoPR

Figure 7

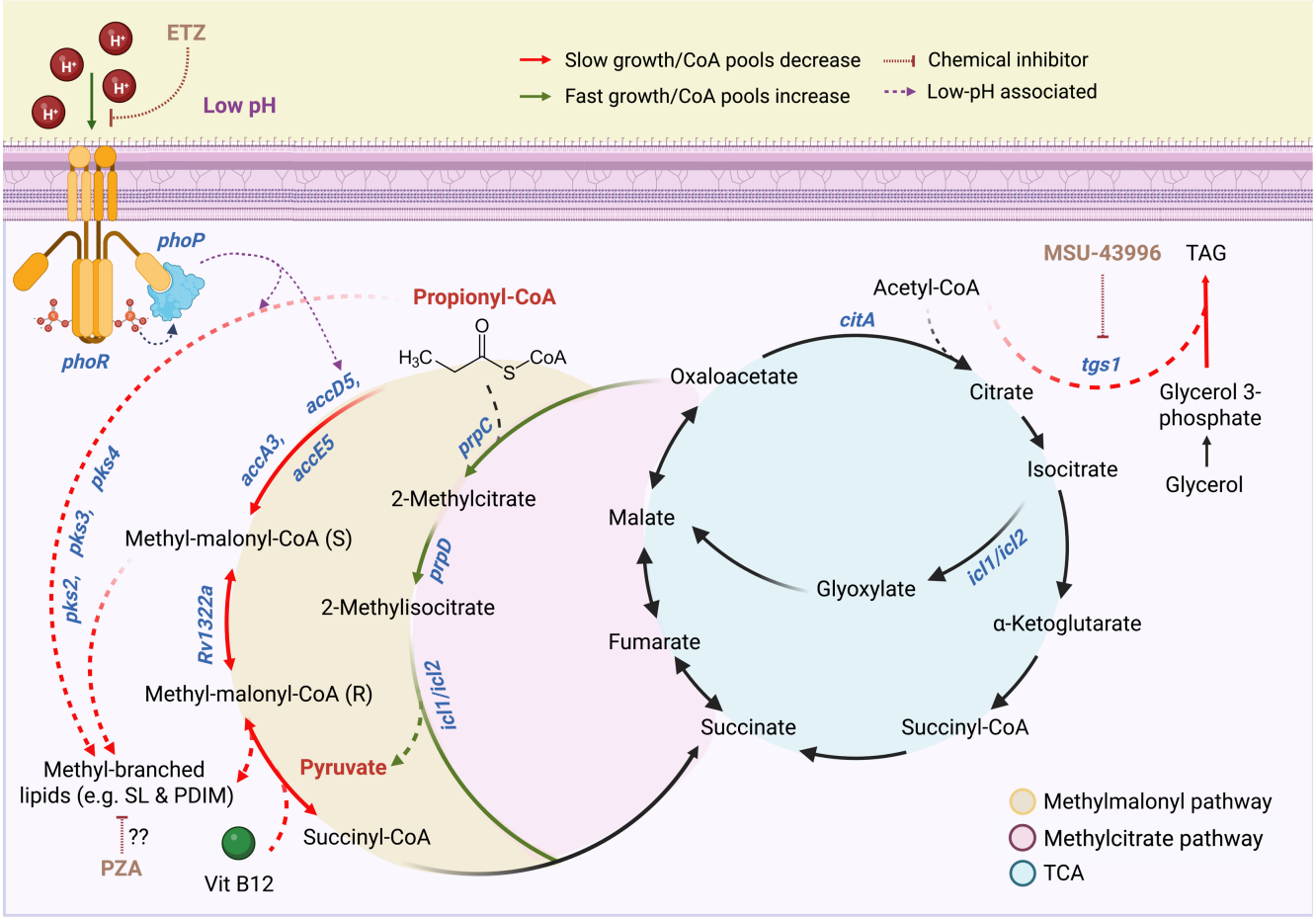
ETZ
Low pH
Slow growth/CoA pools decrease
Fast growth/CoA pools increase
Chemical inhibitor
Low-pH associated
phoP
phoR
Propionyl-CoA
MSU-43996
TAG
Acetyl-CoA
citA
tgs1
Glycerol 3-phosphate
Glycerol
Oxaloacetate
Citrate
Isocitrate
Malate
Glyoxylate
icl1/icl2
α-Ketoglutarate
Fumarate
Succinate
Succinyl-CoA
accD5,
accA3,
accE5
prpC
2-Methylcitrate
prpD
2-Methylisocitrate
Methyl-malonyl-CoA (S)
Rv1322a
Methyl-malonyl-CoA (R)
pks2, pks3, pks4
Methyl-branched lipids (e.g. SL & PDIM)
??
PZA
Vit B12
Pyruvate
Succinyl-CoA
Methylmalonyl pathway
Methylcitrate pathway
TCA

Figure 8

Supplemental Table and Figures

Mycobacterium tuberculosis growth arrest on propionate at acidic pH is suppressed by mutations in *phoPR* and pyrazinamide treatment

Heather Murdoch[1,2], Shelby J. Dechow[1,2], Bassel J. Abdalla[1] and Robert B. Abramovitch[1]

[1]Department of Microbiology, Genetics & Immunology, Michigan State University, East Lansing, MI,48824

[2]Co-first authors contributed equally to this study.

Supplemental Table

Table S1: Transposon Mutant Propionate Selection Summary

Supplemental Figure Legends

Figure S1. Bacterial Growth and viability of WT, Δ*phoPR* mutant, and complemented strains grown on propionate and treated with MSU-43996 at neutral pH. A) bacterial growth of the three strains on propionate at pH 7.0, showing no significant differences in growth rate. B) bacterial growth of the three strains on propionate at pH 7.0, treated with MSU-43996 or the vehicle, showing no major differences in growth rates based on strain or treatment.

Figure S2. PhoPR restricts growth at acidic pH by diverting carbon from the methyl citrate cycle. A) CFUs from the corresponding experiment in Figure 5A, showing cell death in the ETZ treated icl2 and icl1/2 knockouts. **B)** CFUs of Vitamin B12 treated Mtb strains. **C)** CFUs for figure 5C showing enhanced growth of MSU-43996 treated Mtb. **D**) Vitamin B12 does not impact the growth of strains at neutral pH. A one-way ANOVA was used for the viability experiments, * <0.05, ** <0.01, *** <0.001, **** <0.0001. Experiments were replicated at least twice with similar results.

Figure S3. Function of Icl and PhoPR at neutral pH on propionate. Growth of Mtb strains at pH 7.0 on propionate. ETZ did not impact growth in the *Icl1* or *Icl2* single mutants. The double icl1/2 mutant dies due to propionate toxicity. An unpaired t-test was used between individual groups for the growth curves, * <0.05, ** <0.01, *** <0.001, **** <0.0001. Experiments were replicated at least twice with similar results.

Figure S4. Itaconic acid inhibits enhanced growth of the Δ*phoPR* mutant. Itaconic acid inhibits the ability of the Δ*phoPR* to grow on propionate at pH 5.7. An unpaired t-test was used between individual groups for the growth curves, * <0.05, ** <0.01, *** <0.001, **** <0.0001. Experiments were replicated at least twice with similar results.

Figure S5. Free CoA pools on glycerol as a sole carbon source. During acid growth arrest on glycerol, all three strains maintain relatively low free CoA pools. Two-way ANOVA was used for this analysis, * <0.05, ** <0.01, *** <0.001, **** <0.0001. Experiments were replicated at least twice with similar results.

Figure S6. Vitamin B12 inhibits enhanced growth of WT Mtb treated with PZA. The inhibition of enhanced growth is consistent with PZA inhibiting lipid synthesis to promote growth, as making another lipid synthesis pathway available abolishes enhanced growth. Multiple comparison unpaired t-test was used for the analysis between treatments and the control, and between strains receiving the same treatment, * <0.05, ** <0.01, *** <0.001, **** <0.0001. Experiments were replicated at least twice with similar results.

Figure S7. Vitamin B12 inhibits enhanced growth of WT Mtb treated with PZA. CFU data for OD data presented in Figure S6.

Figure S8. Sensitivity of Mtb to PZA on Pyruvate as a sole carbon source at pH 5.7. PZA treatment does not result in enhanced growth with pyruvate as a sole carbon source.

Figure S9. PZA suppresses acid growth arrest on propionate in Mtb Erdman. To determine if the enhanced growth by PZA is conserved across strains, the PZA treatment experiment from Figure 7 which as conducted in CDC1551, was repeated in Mtb Erdman. Multiple comparison Unpaired t-tests were used for the growth assays, and one-way ANOVA was used for the viability assays, * <0.05, ** <0.01, *** <0.001, **** <0.0001. Experiments were replicated at least twice with similar results.

Figure S10. Sensitivity of Mtb to PZA treatment at pH 7.0. Control experiment for data in Figure 7, showing PZA is not active on Mtb grown in propionate at pH 7.0.

Table S1: Transposon Mutant Propionate Selection Summary

Mutant #	Approx AT or TA site/gene length (nt)	MT number	Rv Number	Gene Number	PDIM Mutation?
1.1	416/1458	MT0783	Rv0758	*phoR*	None
1.2	159/1458	MT0783	Rv0758	*phoR*	None
1.4	311/744	MT0782	Rv0757	*phoP*	None
2.1	278/1458	MT0783	Rv0758	*phoR*	*ppsE*
2.4	145/1458	MT0783	Rv0758	*phoR*	*ppsE*
3.2	145/1458	MT0783	Rv0758	*phoR*	*ppsE*
3.3	1124/1458	MT0783	Rv0758	*phoR*	*ppsE*
3.4	416/1458	MT0783	Rv0758	*phoR*	*ppsE*
4.1	378/1458	MT0783	Rv0758	*phoR*	*ppsE*
4.2	378/1458	MT0783	Rv0758	*phoR*	*ppsE*
4.3	416/1458	MT0783	Rv0758	*phoR*	*ppsE*
4.4	416/1458	MT0783	Rv0758	*phoR*	*ppsE*

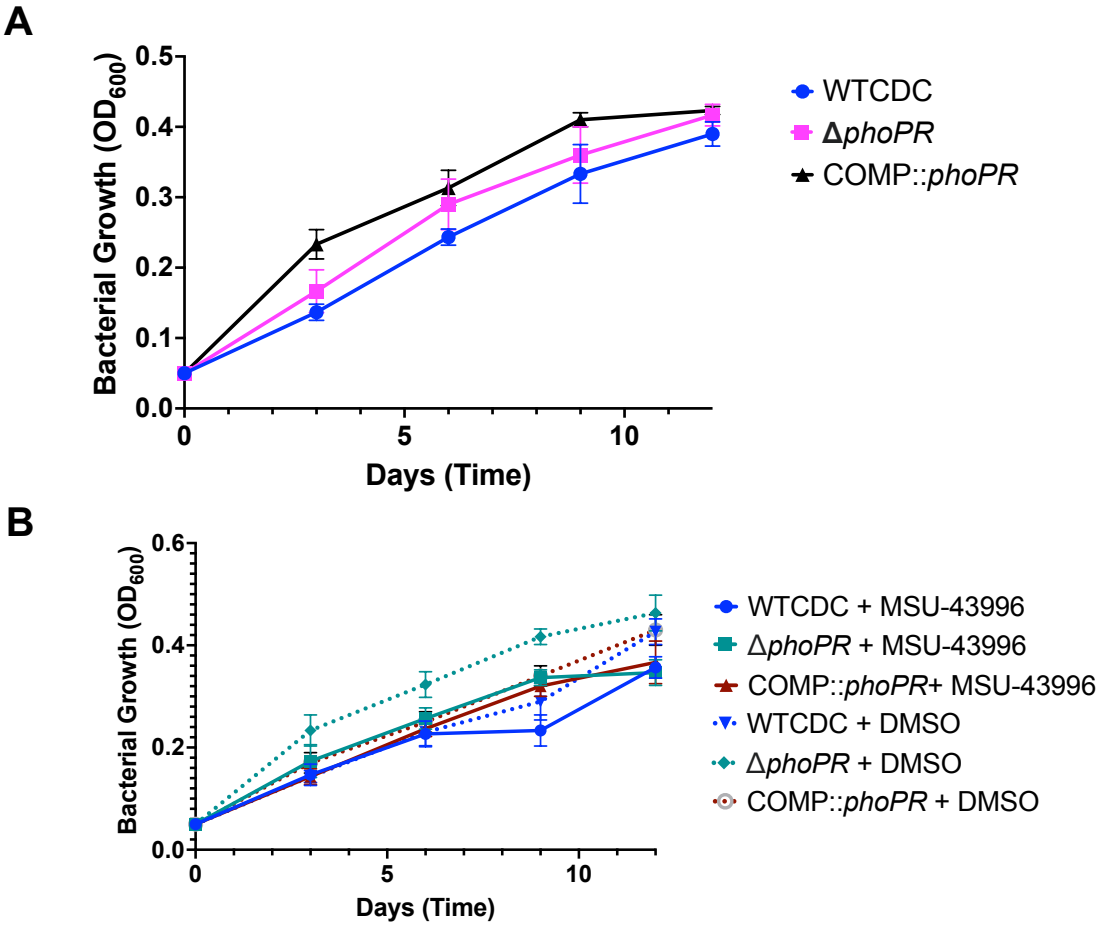

Supplemental Figure 1

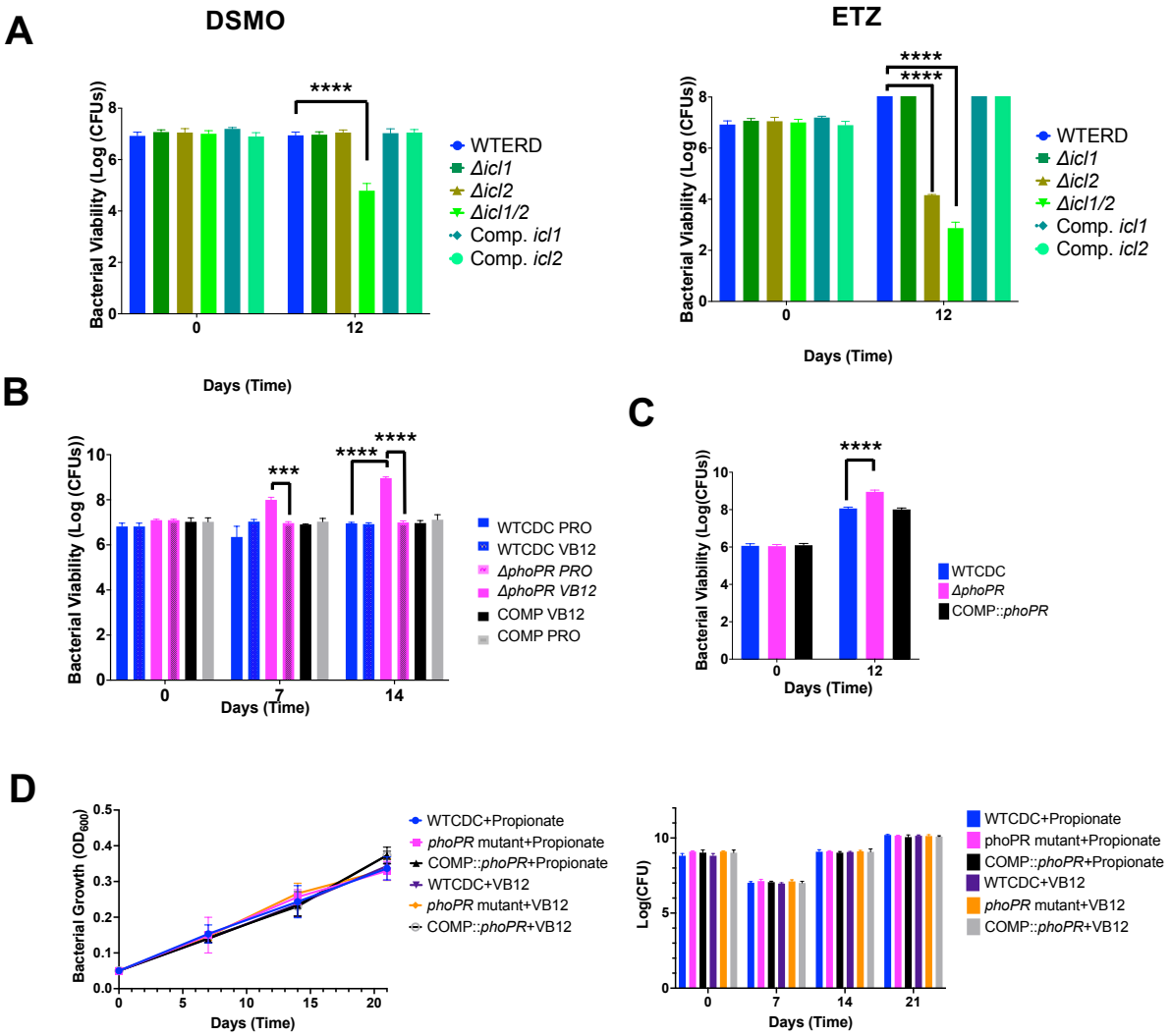

Supplemental Figure 2

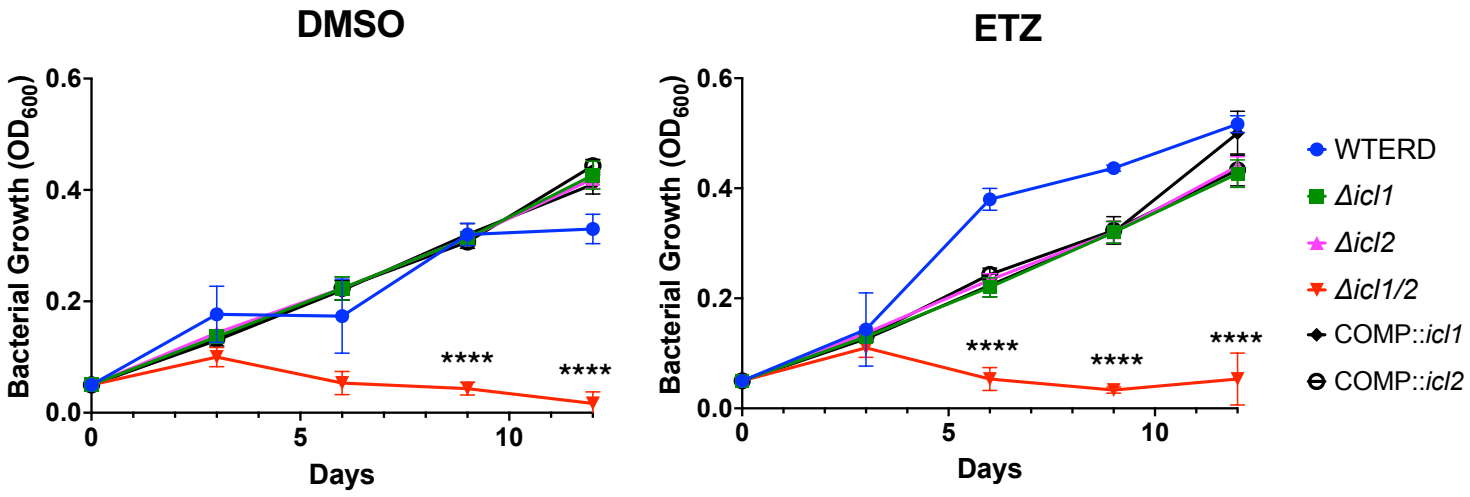

Supplemental Figure 3

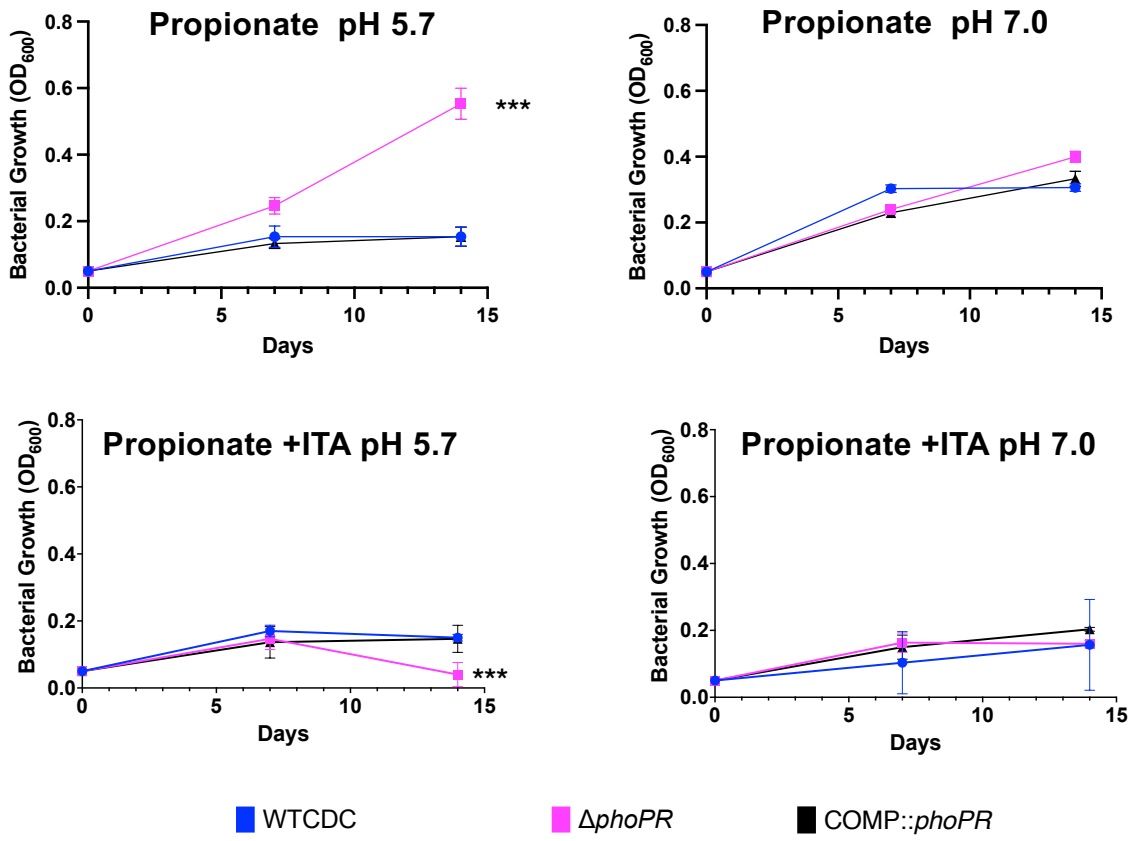

Supplemental Figure 4

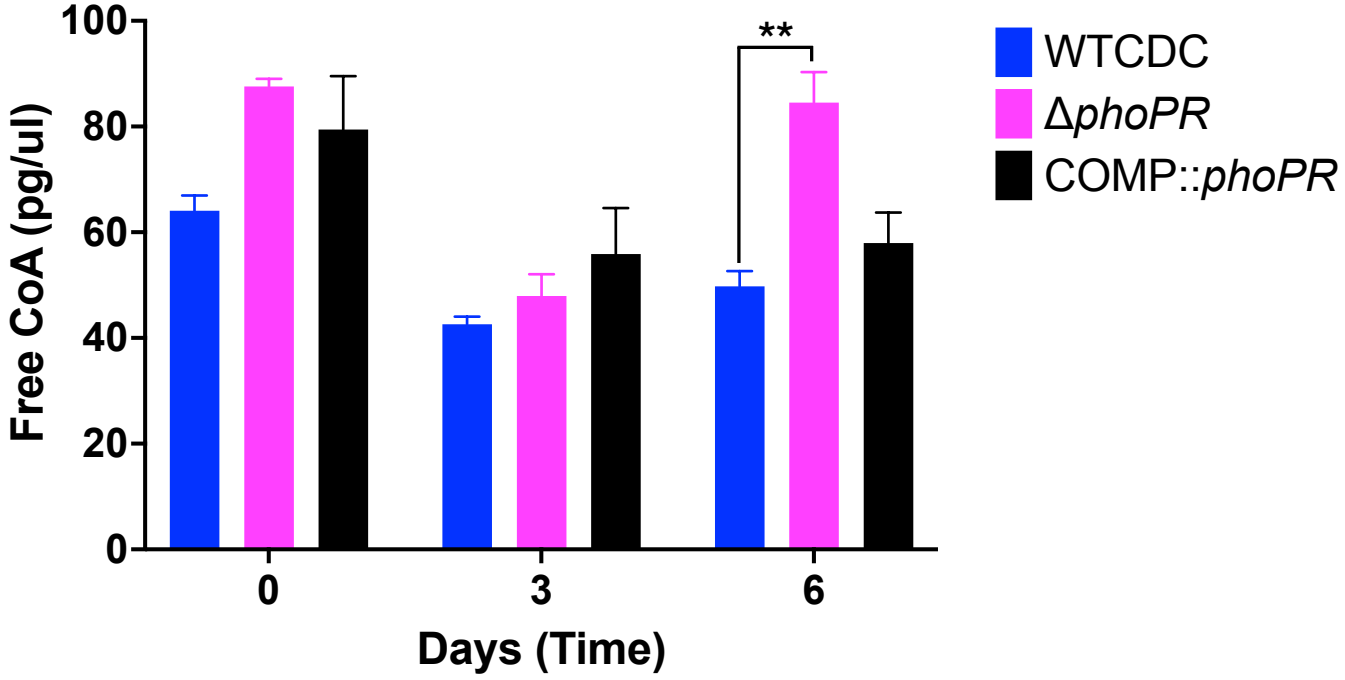

Supplemental Figure 5

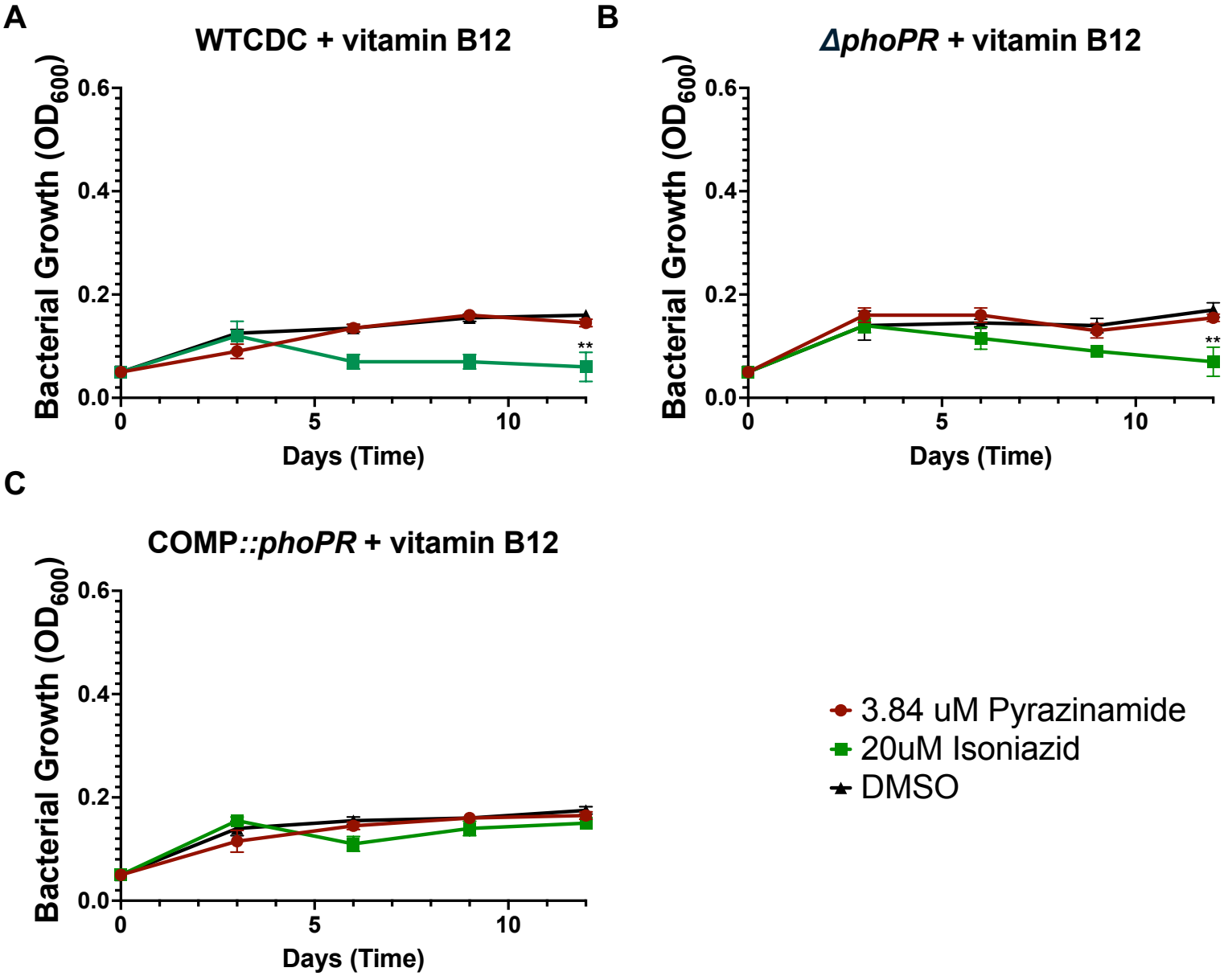

Supplemental Figure 6

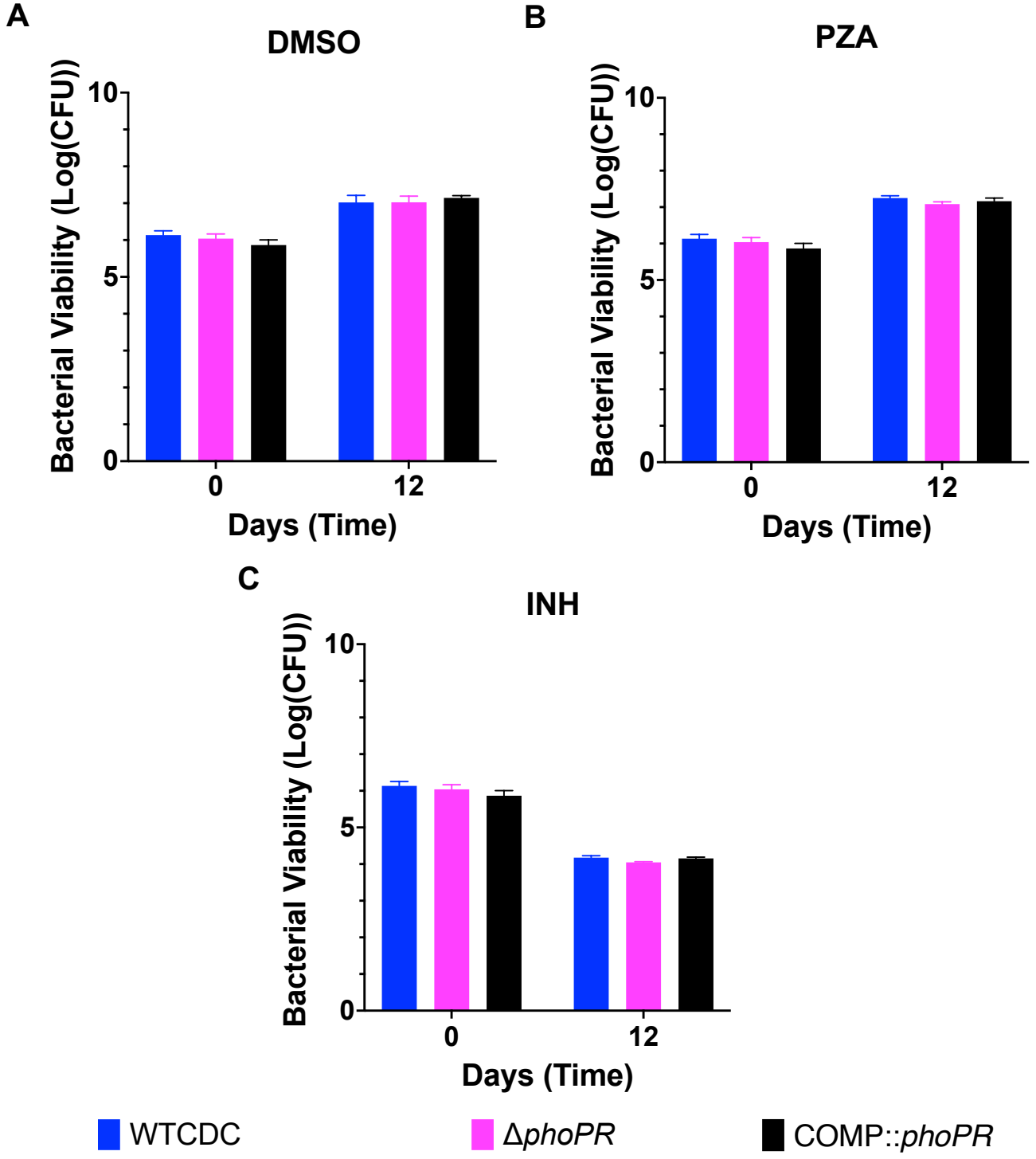

Supplemental Figure 7

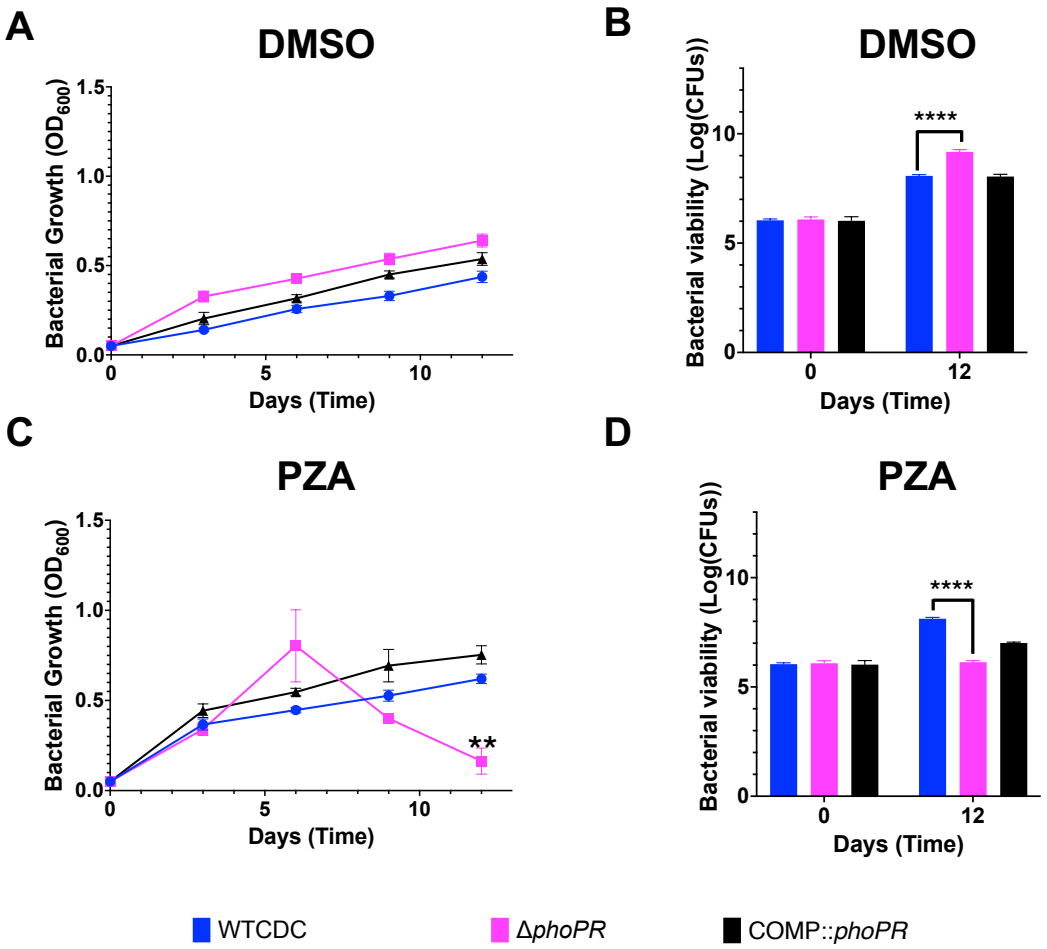

Supplemental Figure 8

A

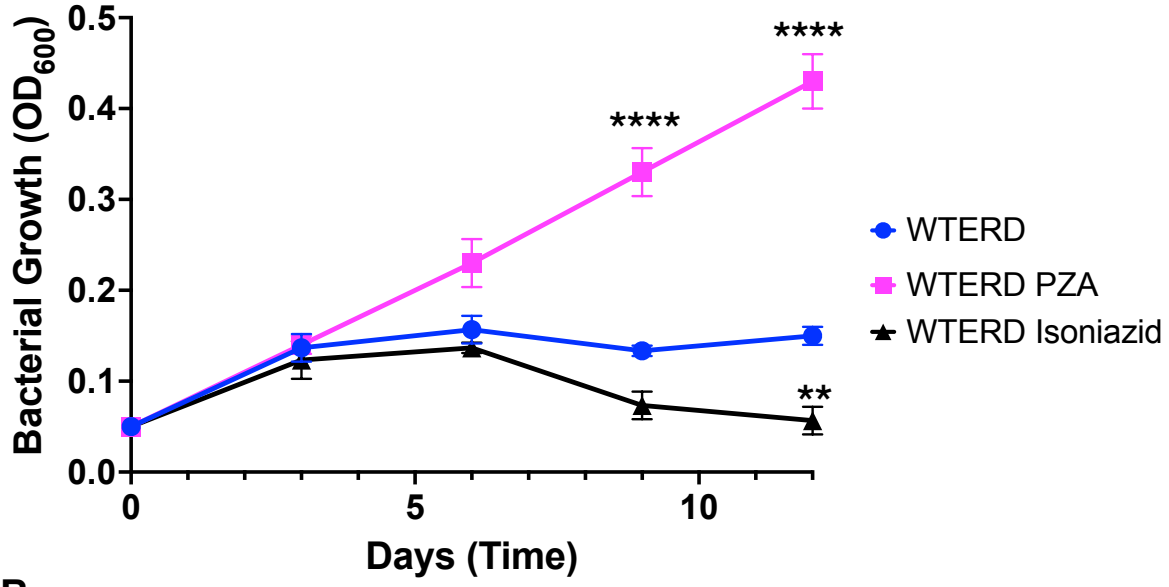

B

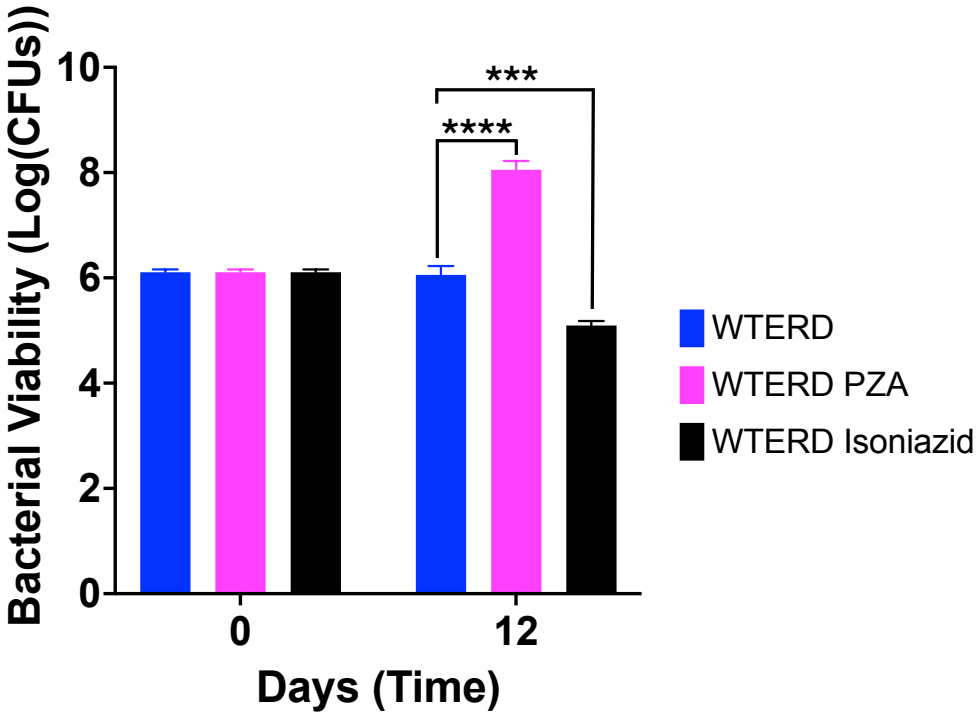

Supplemental Figure 9

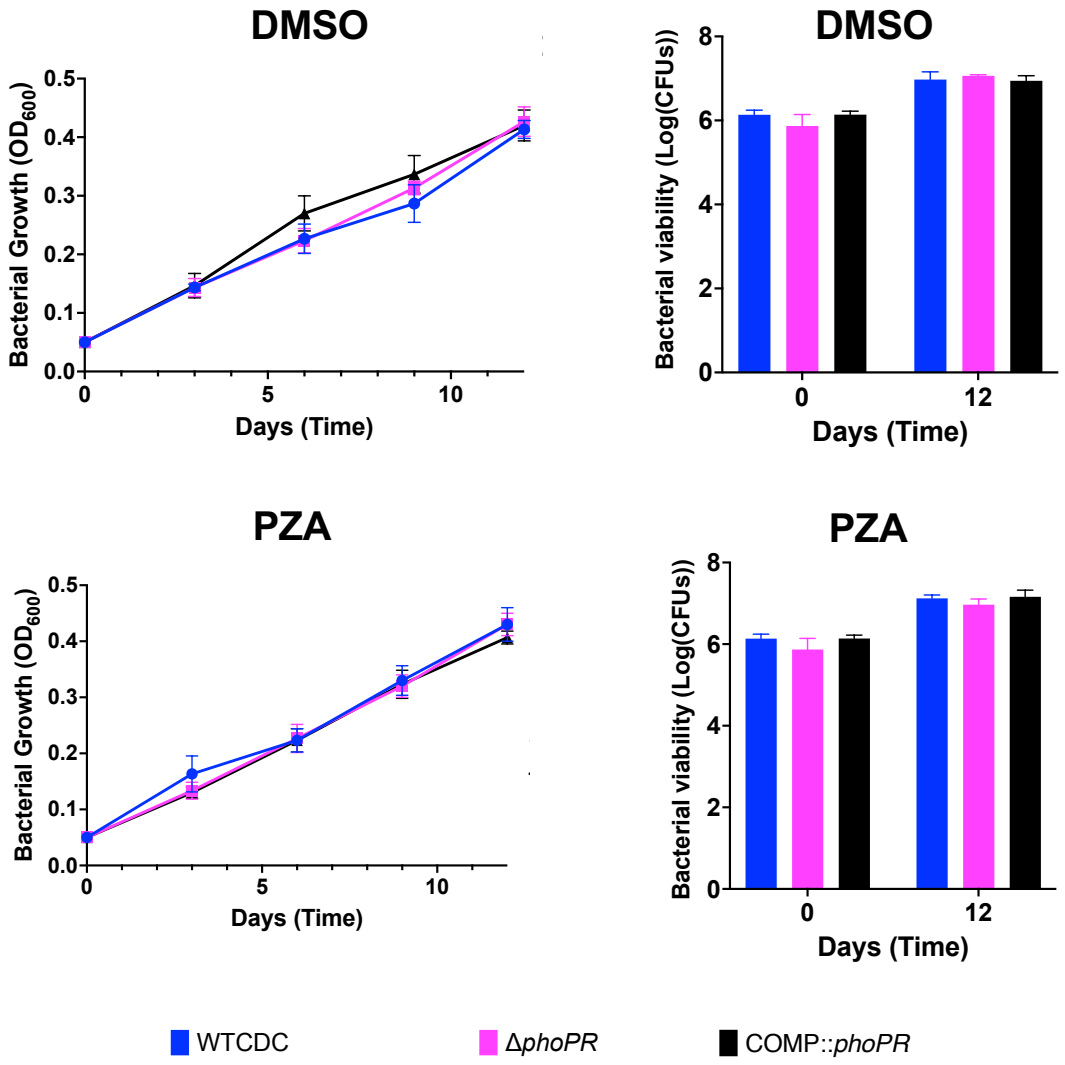

Supplemental Figure 10